

EFFECT OF LOW CONSTANT DIRECT CURRENTS ON
QUASI-STATIC MECHANICAL RESPONSE OF
CARBON FIBER POLYMER MATRIX COMPOSITES

By

RAVI RAJA NAIDU AKULA VENKATA

Bachelor of Science in Mechanical Engineering

Vasavi College of Engineering

Hyderabad, Telangana

2010

Submitted to the Faculty of the
Graduate College of the
Oklahoma State University
in partial fulfillment of
the requirements for
the Degree of
MASTER OF SCIENCE
May 2018

EFFECT OF LOW CONSTANT DIRECT CURRENTS ON
QUASI-STATIC MECHANICAL RESPONSE OF
CARBON FIBER POLYMER MATRIX COMPOSITES

Thesis Approved:

Dr. Raman P. Singh

Thesis Adviser

Dr. Ranji Vaidyanathan

Dr. Khaled Sallam

ACKNOWLEDGMENTS

I am grateful to my faith in God which has kept all delays at bay and pushed me towards successful completion of the thesis. I am very much thankful to my advisor, Dr. Raman P. Singh for having immense trust in my abilities and guiding me through the ups and downs of research. I was always encouraged to come up own ideas, but was driven in the right direction whenever needed.

I would also like to thank rest of the thesis committee members Dr. Ranji Vaidyanathan and Dr. Khaled Sallam who were kind enough to give me time for discussions and suggestions on this research project.

I would also lovingly acknowledge friends and fellow lab mates in the MAML group including Dr. Kunal Misra, Libin K Babu, Shamim Mondal, Blaze Heckert and Victor Ornelas Perez for their kind inputs and support. Their enthusiasm, optimism and energy levels created a very cheerful and lively atmosphere in the lab.

I am very thankful to fellow HRC members Dr. Malay Jana, Vishal Yeddu, Ranjan Singhal, Padmanapan Rao, Vishant, Dilli and Jonathon whose company I relished thoroughly.

I wish to thank my parents and relatives for believing in my strength and continuously cheering my success over the years.

Name: RAVI RAJA NAIDU AKULA VENKATA

Date of Degree: MAY, 2018

Title of Study: EFFECT OF LOW CONSTANT DIRECT CURRENTS ON QUASI-
STATIC MECHANICAL RESPONSE OF CARBON FIBER POLYMER
MATRIX COMPOSITES

Major Field: MECHANICAL AND AEROSPACE ENGINEERING

Abstract: Carbon-fiber reinforced composites (CFRP) can be subjected to two different levels of direct current conduction, either under catastrophic high current conditions such as lightning-strike on an aircraft structure or under low constant current conditions as in multifunctional composite structures used for resistive heating, energy harvesting and distribution. While the effect of high currents for short durations on mechanical properties of CFRP are well studied, effects of long-term exposure to relatively low constant direct currents are studied less. The focus of this study is to measure the change in mechanical properties of CFRP subjected to constant low direct current of different intensities and durations. In the present investigation sixteen ply unidirectional CFRP laminates made of IM7 carbon fiber and Diglycidyl ether of bisphenol-F (DGEBF) based epoxy are fabricated using vacuum assisted resin transfer moulding (VARTM) technique. Samples of two different sizes namely coupon (127 mm x 12.7 mm) and plate sizes (254 mm x 177.8 mm) are snug fitted between copper electrodes along the fiber direction and are exposed to two different levels of electric current intensities (0.062 A/mm^2 and 0.093 A/mm^2) under constant direct current mode for three and six hours. The corresponding change in the voltage which is direct measure of change in resistance of the sample is recorded and logged in a spreadsheet with the help of a BASIC based power supply instruction code. Conduction path within the composite sample is mapped by measuring and logging its surface temperatures continuously using far infrared sensor array (16 x 4 resolution) within a total field of view of $120^\circ \times 30^\circ$ across entire width of the sample at mid-length. Subsequently, the mechanical properties of samples corresponding to current exposed, oven heated and as-is conditions are tested as per ASTM D6641 (combined loading compression test) to determine and compare the maximum compressive strengths. Glass transition temperatures which is a reliable indicative of polymer strength is measured using Differential Scanning Calorimetry (DSC) for all categories of exposure namely, current exposed, oven heated and as-is samples. Compression strength results have shown no significant change for all kinds of exposure. Voltage-time curves indicate a linear increase in the resistance of the current exposed CFRP sample. However, there is a lot of noise in the voltage history plot which is apparently due to the hotspot formation at the electrode and sample interface. Temperature history plots show a very slow rate of linear increase in temperatures. Glass transition temperatures support the 'no change' claim by maximum compression strength results by indicating no percentage change in glass-transition temperatures of as-is, current and oven exposed sample

TABLE OF CONTENTS

Chapter	Page
I. INTRODUCTION.....	1
1.1 High intensity direct current studies on CFRP	3
1.2 Low intensity direct current studies on CFRP	7
1.3 Objective	11
II. MATERIALS, EXPERIMENTAL SETUP AND METHODOLOGY	14
2.1 Materials	14
2.2 Sample preparation	14
2.3 Electrical experimentation setup.....	18
2.4 Experimentation method.....	25
2.5 Combined loading compression.....	27
2.6 Differential scanning calorimetry (DSC)	28
2.7 Density and Fiber volume	30
III. RESULTS AND DISCUSSION	32
3.1 Voltage history profile	32
3.2 Temperature history profile	37
3.3 Maximum compression strength	45
3.4 Glass transition temperature	47
IV. CONCLUSION.....	49
REFERENCES	53

LIST OF TABLES

Table	Page
2.1 Design of dc exposure experiment.....	26
3.1 Compression strength for 3,6 hours at constant current 0.062A/sq mm.....	45
3.2 Compression strength for 3 hours at constant current 0.093A/sq mm.....	46
3.3 Tg comparison for all exposures.....	48

LIST OF FIGURES

Figure	Page
1.1 Current waveform (ARP5412B standard)	4
2.1 Schematic of VARTM setup.....	17
2.2 VARTM setup.....	18
2.3 Schematic of electric test setup.....	19
2.4 16*4 Melexis multiarray sensor.....	21
2.5 Circuit breakout for IR sensor.....	21
2.6 Monitor display of thermal pixel information	22
2.7 Schematic of Electric fixture	23
2.8 Real-time of Electric fixture	24
2.9 Combined Loading Compression (CLC) Test Fixture.....	28
3.1 Voltage history for 3 hours at constant current: 0.062 A/mm ²	33
3.2 Voltage history for 6 hours a constant current: 0.062 A/mm ²	34
3.3 Voltage history for 3 hours at constant current: 0.093 A/mm ²	36
3.4 Temperature history for 3 hours at constant current: 0.062 A/mm ²	37
3.5 Schematic of temperature multiarray (16 x 4 pixel)	38
3.6 Temperature history for 6 hours at constant current: 0.062 A/mm ²	39

3.7	0.062 A/sqmm, Temperature(avg) vs time (3 hrs), coupon size.....	40
3.8	0.062 A/sqmm, Temperature(max) vs time (3 hrs), coupon size.....	41
3.9	0.062 A/sqmm, Temperature(avg) vs time (6 hrs), coupon size.....	42
3.10	0.062 A/sqmm, Temperature(max) vs time (6 hrs), coupon size.....	42
3.11	Temperature history for 3 hours at constant current: 0.093 A/mm ²	43
3.12	Temperature gradient for 3 hours at constant current: 0.093A/sq mm	44

CHAPTER I

INTRODUCTION

Multifunctional composite structures have gained tremendous traction since late 20th century. The prime reason being the promising commercial and performance potential offered by such composites. It has now become almost inevitable to rigorously study the wide variety of benefits that such engineered materials can offer to industries like aerospace, autonomous on land vehicles and unmanned underwater vehicles [1] DARPA's morphing aircraft structures program [2] and General Motor's Autonomy Concept [3], NRL developed structure-battery composites for use as hull structure on electric unmanned underwater vehicles (UUVs) [4] stand as perfect examples to the future what multifunctional composites hold. Conventional approach to design modern structures is to design its load bearing functionality and other functionalities separately. Such an approach is parasitic as it results in less efficient load bearing that pays penalty for added weight due to attachments which perform non-structural functions separately. Therefore, there is a need for multifunctional synergistic structures that have non load bearing functionalities integrated to load bearing functionality in order to respond effectively to multiple stimuli. Multifunctional composite structures have less weight to volume ratio and hence there is more flexibility in design size. They have better performance to weight ratio which implies higher efficiency. Additionally, cost, power consumption and complexity of overall system invariably drops compared to regular structures. Safety and versatility of multifunctional composite structures are significantly high. Their utility is more interdisciplinary than any other material known. Multifunctionality within a

material can be developed on several dimensional scales with increasing interaction between phases and engineering complexity as the scale goes down in size. Matic et al [5] has categorized the different listed materials scales into three types. Type 1 material is comprised of phases in which one phase is simply mounted, coated, or laminated on the other phase, usually a structural component. Type 2 materials have distinct phases in which one function is plugged into another phase, usually a structural component. Type 3 materials are truly interwoven materials in which the phases of each material are interlinked so that the physical separation between phases becomes less obvious. The true potential of multifunctional materials to performance-tailored structures is found in Type 3 materials. All these attributes create a natural demand for these structures in commercial applications.

Multifunctional composites have found its application in multiple recent cutting edge technologies and commercial applications including structural functions such as mechanical properties including strength, stiffness, fracture toughness, and damping, while non-structural functions include electrical and/or thermal conductivity, sensing and actuation, energy harvesting/storage, self-healing capability, electromagnetic interference (EMI) shielding, recyclability and biodegradability [6]. Carbon fiber reinforced composites are one such class of multifunctional composites that can provide with a variety of benefits to the structure due to its variety of superior properties exhibited by its in plane strength, stiffness, thermal and electrical properties. Traditionally carbon fiber reinforced polymers (CFRP) were introduced to the aerospace, automobile and civil engineering industries for their high strength and low weight. Luo and Chung et al [7] discussed about the idea of using carbon fiber polymer matrix composites as capacitors. They found that CFRP can act as a parallel plate capacitor with very high specific capacitance with slight modifications in its fabrication. The fact that military fighter plane, F-22 commissioned in 2005 uses about 25% CFRP composite materials by weight while Boeing has built its next generation passenger airplane (787) using CFRP composites at approximately half the

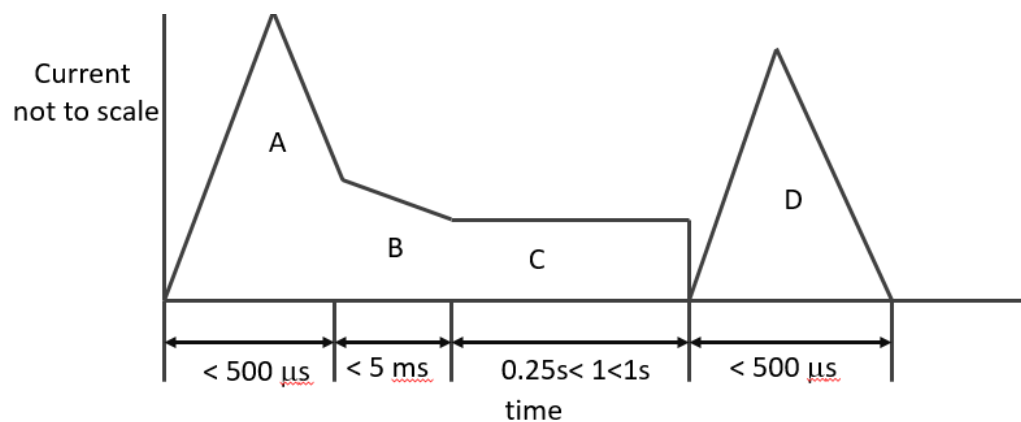
material weight [8] exemplifies the fact that aerospace industry especially relies on its structures to be as efficient as possible and CFRP can be seen as one of those engineered materials which can fulfill this demand. However, traditional CFRP has relatively poor electrical and thermal conductivities as a consequence of the bulk insulating polymer matrix. Additionally, CFRP is by nature non-isotropic in its properties, especially mechanical, thermal and electrical properties. Although the in-plane electrical and thermal conductivities are greater than the out-of-plane directions, they are still comparatively poor and can act as an impediment to the applications of the material. Consequently, it is of prime interest to impart electrical and thermal functionalities in the in-plane and the out-of-plane directions of the CFRP [9]. Several researches have done number of studies on improving the thermal and conductivity of CFRP using various techniques that include method of fabrication and constituent material selection. However, there is an important challenge in the way of these developments. The electrical conductivity mechanism within the constituents of a multifunctional composite is to be studied well enough to check if it is not interfering with mechanical strength overall [1]. Enough study hasn't been done to check the mechanical response of CFRP subjected to electric currents. Therefore, this study forms this knowledge gap as the basis to make some initial strides in investigating this problem.

1.1 High intensity current studies on CFRP

Best case for high current study on CFRP are studies on simulated lightning protection of CFRP. Desire to construct more and more efficient aero-structures has laid emphasis over increased usage of polymer composite structures instead of conventional metallic aero-structures. However, compared to the aluminum alloys the CFRP has very weak electrical and thermal conductivity. This makes the CFRP structures very susceptible to lightning strikes. Also less conductive CFRP allows electromagnetic field to penetrate through it.

Lightning to an aircraft is rare, but it is assumed that a transport aircraft is hit once a year. For commercial aircraft, lightning strike occurs between the first 1,000 and 10,000 hours of flight, which is equivalent to once every year. Most lightning strike occurrences do not result in catastrophe, however, there were a total of 40 lightning related aircraft accidents between 1963 and 1989. In addition, 8% of wind turbines are struck by lightning every year, but 80% of wind turbine insurance claims are lightning strike related.

The environment and test current waveforms defined in SAE aerospace recommended practice ARP5412B as shown in figure 1.1 are the best lightning data and analysis currently available for aircraft analysis and testing for lightning strike protection [10].



Component A (First Return Stroke):
 Peak Amplitude : 200 kA
 Time duration : less than 500 micro seconds

Component B (Intermediate Current):
 Peak Amplitude : 2kA
 Time duration : less than 5 milli seconds

Component C (Continuing current):
 Peak Amplitude : 200--800 A
 Time duration : 0.25—1 sec

Component D (Subsequent return stroke):
 Peak Amplitude : 100 kA
 Time duration : less than 500 micro seconds

Figure 1.1 Current waveform (ARP5412B standard)

Zoning criteria as shown in the figure depicts the current component rating over a transient time scale. Zoning concept had been conceived to assess the damage accordingly [12]. Indirect effects of direct continuing currents trying to ground themselves through Zone 3 (A+C) of an aircraft mainly affect the front and rear wings of an aircraft. The indirect effects consist of branched out electric currents of very low magnitudes. The component C is characterized to be of low intensity constant current as compared to rest of high current transient nature. This particular component is primarily responsible for more direct charge transfer to rest of the aero structure parts for a longer period in a relative time scale. Therefore, the danger from constant direct current discharges for a brief period of time have to be seen as a considerable threat to the durability of certain portions of an aircraft made of CFRP. The zone within which the lightning stroke is active is called a stroke zone and time taken by one stroke to sweep across such a zone is called attachment time. These attachment times are relatively small in the order of milliseconds and basically depend on the velocity of the aircraft and the type, thickness of the dielectric covering the skin of an aircraft. If the attachment time is higher, then it means high charge transfer or conduction is taking place. This parameter is very important as it is crucial to deciding when the aero-metallic body is going to puncture. When an electric lightning strikes an aero plane an entry and exit point are formed where the lightning leader tip has its direct effects. As the distance between the entry and exit point increases, then the electric field potential between them also increases. This very much depends not only on the electric potential equations on a moving plane, but also on the conductivity properties of the dielectric through which the field passes. This is very different for different areas within an aircraft body. The damage caused by these currents is so high that its visibly detectable and requires a major overhaul. The current components B and C although relatively lower in amperage also cause considerable damage to the aircraft making repair very much necessary. It's important to answer the question that if CFRP are used instead of aluminum body covered in copper mesh would that influence the existing damage zones. If the answer is yes, then what would the

consequences be is also an interesting question to answer. Significant amount of the research done in comparing the change in the attachment point within an aero-structure compared to conventional metal structures which said that there is no significant change.

Hence, the only question is how would a polymer composite respond to a lightning stroke. Lightning strike causes damage to airframe structures by several different physical mechanisms. Flowing electric energy is dissipated by any conducting system primarily as joule resistive heating. The degree of joule heating is represented by an important parameter named action integral which is a first degree approximation the integral of the current squared over time. It is higher for A, D high peak transient current segments. More the joule heating more is the volume heating within the polymer matrix composite. The zone C however has the highest direct charge transfer over the relatively longer time in the transient time scale.

CFRP is anisotropic in many ways. Properties like thermal coefficient of expansion, electrical and thermal conductivities are direction dependent. In few directions the electric conductivity of CFRP is three orders lower compared to that of conventional metal (resistivity of carbon fiber is 14.97×10^{-3} ohm-mm). Joule heating due to transient currents in CFRP compared to aluminum is significantly higher. This is because of presence of heat producing carbon fiber and heat absorbing polymer matrix which tends to accumulate heat. For transient currents, Joule heating is higher compared to the direct heat energy deposited into the structure by the electric arc alone. Therefore, the reduction in electric resistance is the most important thing to reduce the consequent damage. The desired resistance would be to generate as much less heat as possible taken care not to degrade the surrounding polymers due to high temperatures.

Other thermal effect damages in the case of lightning strike include direct heat input from the hot plasma channel and thermal radiation from the hot plasma channel. Transient mechanical force oriented damage mechanisms include shock waves from the supersonic expansion of the hot plasma

channel [13], magnetic volume forces, shock waves caused by exploding materials. The important question to be asked within the present investigation is how the above damage mechanisms change with respect direct currents which are constant and low in magnitude.

Compression strength degradation after lightning strike was studied for five different lightning strike protection configurations by Mall and Ouper et al [14]. These configurations consisted of a ply of nickel-coated carbon woven fabric as lightning strike protection component besides the four plies of standard carbon fibers (AS4) fabric embedded in the epoxy (EPON 862). The other four systems had an additional protection system, which was nickel-nanostrand veil (NiNS), aligned buckypaper, random buckypaper, or mixed buckypaper made up of vapor-grown carbon fibers and single-walled nanotubes. All other buckypapers were made of single-walled nanotubes. All five systems were tested under monotonic compression to measure their ultimate compressive strength before and after a simulated lightning strike. There was considerable reduction from the lightning strike, which ranged from about 75% to 30%. The reduction was maximum (75%) in the case of NiNS and minimum with RBP (30%). NiNS was the most conductive material and buckypapers were the least conductive materials. Overall, damage from the lightning strike or the high intensity current studies seems to be related to the conductivity of protection system. This makes researchers think and ask if low direct currents have the same detrimental effect on CFRP as that of high currents or not.

1.2 Low intensity current studies on CFRP

The nature of studies so far that have attempted to study influence of low intensity direct constant electric currents on CFRP are limited to study on structural health monitoring of in service CFRP, study on anisotropic electrical properties of CFRP and study on impact response. The study on change of quasi static mechanical response of CFRP exposed to low direct currents is not only important in a technological standpoint but also in a commercial aspect for example CFRP is used

as resistivity based heating substrate elements in various electronic circuits for heating due to high joule heating.

Structural health monitoring is done on CFRP mostly used in-service air craft structures and wind turbines. This is based on the piezo resistivity property of CFRP [15]. Piezo-resistivity is the resistance change with changing strain. Whenever there are fiber breakages or deformation in a unidirectional CFRP there is a corresponding change in the resistance which is sensed and registered as equivalent degree of damage to a structure. Tensile test was done to introduce the strain in single and mutli ply CFRP. Four probe method was used to sense the change in the resistance. The effect of shear loading was also investigated this way. Results showed that CFRP in fiber direction has a positive gage factor and the value is 2. Piezoresistivity of CFRP in transverse direction has a positive gage factor against applied tensile load. The gage factor is 4 when the load is applied in the transverse direction. Shear loading has no effect on the electrical resistance change.

Surface Crack Detection for Carbon Fiber Reinforced Plastic (CFRP) Materials Using Pulsed Eddy Current Thermography is a Nondestructive technique to detect the notches within a CFRP sample but identifying the change within the heating pattern and transient temperature changes [16]. It has been established that pulsed eddy thermography is a very effective method to detect surface cracks or notches on a conducting polymer matrix composite like CFRP. Application of small electric potentials to detect the delamination in CFRP is a nondestructive method to identify the degree of mode1 and mode2 delamination by sensing the change in through thickness electric resistance [17]. This method came as an alternative to constant direct current thermography techniques which rely on built-up temperatures that take time to stabilize. All these methods involved small constant direct currents to pass through CFRP with an assumption that the flowing current would have negligible or no effect by itself on the mechanical properties of CFRP. However, this assumption has to be tested and there are no studies so far done to check these assumptions.

Several of experimental and numerical studies have been carried out on unidirectional CFRP in order study the anisotropy of electrical properties of CFRP. In this study the CFRP is considered as an electrical percolation system with conductive carbon fibers touching each other width wise and non-conductive matrix system. Conduction studies are done using four probe and ix probe methods for different volume fractions. The correlation between the electric ineffective length which is the length after which every fiber regains its conductivity and measure anisotropy is presented.in this study. This study is validated using numerical studies such as Monte Carlo simulation technique and Kirchhoff rule [18].

In a study by Sierakowski et al [19] influence of electric current on low velocity impact response of unidirectional and cross-ply CFRP subjected to electric currents was studied. Preliminary results have shown that short-term application of electric current leads to an increase in the impact response of the composites and continued application of current leads to negative effects on the impact strength of the composite. The tests have been carried out at 0A, 25A and 50 A direct electric current. It was found that there is an increase in the maximum impact load that a 0-degree oriented sample can take with increasing current intensity. However, this trend is only possible with very less duration such as 25 milli sec of passage of current. Maximum impact load saw a mere 5% increase for 25A current and 8.6% increase for 50A current. In the case of prolonged study, which is impact response taken 36 mins after the passage of current, was found that the maximum load fell as much as 18% for 50A Increase in the maximum impact strength of CFRP subjected to constant direct currents for very short periods of time have been attributed to two reasons. The first reason is mechanical and electromagnetic loads interact in a very complex non-linear way. The stressed state of composite plate is either amplified or counter balanced by the induced electromagnetic field due to passing current based on its intensity and orientation [20]. Also, it is claimed that the material's failure envelope is increased whenever the composite plate is subjected to electromagnetic field and therefore can withstand higher strength [21]. The reason

behind the immediate reduced impact response to the prolonged effect of passage of current has been attributed to the coupling of thermal, mechanical and electromagnetic fields. It is assumed to be a complex dynamic nonlinear problem and is yet to be resolved. Although this study tries to answer questions on impact response, the question about the quasi-static response of CFRP under a prolonged time duration of about 3 to 6 hours remains unanswered.

Haider et al [22] studied the anisotropic electrical behavior of CFRP. For in-plane study a current intensity of 80 kA/m^2 was applied and 6 kA/m^2 was applied for through thickness study. The study is done for different orientation of ply stacking. A 3D X-ray microscope was used to visualize and quantify local material change due to electric current. The study revealed the fact that the electrical properties are dependent on laminate design and fiber orientation in the laminate. Electric current can cause some damage to the matrix. Material state changes are the reasons behind the fact that electrical properties change with passing current. Joule heating was attributed to these material changes. Increased current density can cause irreversible damage to the existing material state of CFRP. CFRP are electrically conductive due to carbon fibers [23]. Carbon fibers are also having high thermal conductivity enough to conduct the current induced temperature rises without burnout. Axial passage of DC in a carbon fiber composite causes Joule effect which is resistance heating induced due to moving electric charges. It can be observed using IR imaging or any temperature sensing devices. If the effect of joule heating is very high and temperatures generated close to the interface between fiber and epoxy matrix are significantly higher, then decomposition of the matrix around the fiber can be observed. There is also a possibility for matrix and fiber debonding at such high temperatures. The third kind of damage is matrix cracking due to electron hopping between close fibers of same carbon ply. Due to the anisotropy of CFRP, different conduction paths are possible within the lamina. This causes electron hopping. The other kind of damage in composites due to high electric currents is delamination. Two possible reasons were assigned to this. Dielectric breakdown in epoxy matrix and uneven temperature gradient across the

thickness of the composite plate causing out of balance thermal expansion/contractions creating stress enough to delaminate plies.

However, this study although shows a visual evidence of damage did not exactly answer the question if these micro damages done to the epoxy could cause considerable decline in the macro-mechanical properties. If the answer is yes, the quantified study over the measure of damage is to be studied. The present study was pursued to investigate the above stated question. Also the influence of duration of current passage on measured damage is to be studied too. Miller and Ferraboli [24] described a phenomenon of Lorentz force where electric current flowing across the opposite clamped ends of a composite plate generates a magnetic field which creates a Lorentz force. These forces may generate local compression in matrix between two fibers and can either strengthen or create matrix cracks in between fibers. This local compression happens mostly during on-axis loading. Although stated in theory, it is still pertinent to ask if such micro changes can effect a macroscopic property like maximum compression strength of a CFRP. This particular question forms the basis of this thesis.

1.3 Objective

The objective of this study is to identify any significant change within any selected macro-mechanical property by passing different current intensities through a carbon fiber polymer matrix with a selected number and orientation of ply. The study has to be carried out for two longer durations in order to finalize if there is any time influence on the level of damage.

The current intensities have been arrived at by test running several 16 ply unidirectional samples and observing the maximum current intensity which is just enough to start burning the epoxy. The two current intensities 0.062 A/mm^2 and 0.0093 A/mm^2 were finalized based on the test runs. Current will be allowed to conduct along the direction of the fiber from one end of the plate to the other. Current conduction shall be attempted to be made uniform between electrode and the

sample interface by application of silver epoxy all along the start and finish conducting cross-sections of the composite plate. This reduces if not eliminate any hot spots generated between sample and electrodes due to which epoxy burnout may be avoided.

Simultaneously, the voltage and current measurements shall be recorded and logged on an excel spreadsheet using a VBA based excel application. Conduction through composite plate is highly unpredictable. It takes random routes whichever are highly conductive and therefore mapping such phenomenon directly is challenging. 16x4 resolution Infrared camera will measure current conduction paths indirectly by identifying the relatively high temperatures on the surface of a conducting composite developed due to electro-thermal effects of flowing electric charges. A 2D array of 64 pixels store and display the temperatures on the plate in its field of view at a very fast rate (4 frames in a sec). Two sets of composite samples are subjected to direct current conduction constantly for about three and six hours respectively. Based on the intensity of current passing through the sample, a unique temperature is expected to develop for each sample on its surface.

Post exposure to current, the composite plates are cut into samples of prescribed dimensions and tested for maximum compression strength under combined loaded compression technique. Compression strengths are compared against their unique corresponding developed surface temperature to see if they follow a trend. Strengths of current exposed samples are compared with only-oven heated samples to see if the temperature alone decoupled from effect of pure current conduction is playing a decisive role in deciding the strength of CFRP.

Glass transition temperatures are good indicators of the strength of a polymer matrix. Highly cross-linked polymer has a higher T_g which means higher strength. Glass Transition temperatures corresponding to each current exposed samples are measured using Digital Scanning Calorimetry (DSC). Post exposure to currents, it is expected that any change in T_g pattern would

strengthen the claims set forth by 0-degree compression test. Voltage history is plotted for 3 and 6 hours respectively to assess and compare the resistance change within the sample. Maximum compression strengths and glass transition temperature values of 3 hours and 6 hours current exposed samples are yet again measured and compared to assess the effect of time duration on the mechanical response of a current exposed-CFRP.

CHAPTER II

MATERIALS AND METHODOLOGY

2.1 Materials

The epoxy resin used in this work is diglycidyl ether of bisphenol F designated by supplier as EPON 862 (made by Miller-Stephenson Chemical Company, Dunbury, Connecticut, USA). It is a low viscous liquid resin made from epichlorohydrin and Bisphenol – F. Its density is 1.17 gm/cc. Curing agent (EPIKURE 3274 made by Miller-Stephenson Chemical Company, Dunbury, Connecticut, USA). It is moderately reactive, low color and low viscous aliphatic amine with a gel time of 135 minutes with density of 0.952 g/cc. Hexcel non-woven, non-stitched unidirectional IM carbon tape made from PAN based 12K carbon fiber tow obtained from CST-The Composite Store, Inc. are used as fiber reinforcement. Carbon content is about 95 % and its density is close to 1.7gm/cc. The fibers are unsized to be independent of any sizing induced electric and thermal property changes and to be chemically compatible with a range of polymer matrices.

2.2 Sample preparation

The present sample preparation setup is a modified VARTM setup adopted from Phillip et al, [25] which implemented a simplified VARTM technique for resin infusion. Vacuum assisted resin transfer molding is a closed mold process that is capable of manufacturing high scale and high performance fiber reinforced polymer structures with very efficient tooling costs[26]. All samples are cut from a 16 ply unidirectional carbon fiber polymer matrix laminate. Every plate of CFRP has two materials mixture of Epon 862 (thermoset resin) and Epikure 3274 (hardener) in mass ratio of

100:40 and 16 plies of unidirectional carbon fiber laminae each of size 355.66 mm x 304.8 mm stacked one over the other.

The fabrication is done by vacuum assisted resin transfer molding (VARTM) inside a fume-hood. It is based on infusing resin mix into the carbon plies taking help of vacuum created within the vacuum bagging chamber with help of a vacuum pump. VARTM system includes glass base, peel cloth, distributor mesh, vacuum bag, resin trap, vacuum pump, resin supply bucket, tacky tape, connectors and flexible tubing. Process first begins with hand lay up of carbon plies hand coated evenly with resin mix and all 16 plies stacked one over each other in fiber direction. This is done very carefully just to ensure that there is no pocket of carbon fiber ply devoid of resin mix. Then the layup is placed on the center of the glass base. A fine layer of parting wax separates the layup and the glass base. Parting wax helps in easy release of the composite plate after it is cured at room temperature. A layer of peel cloth of size 482.6 mm x 431.8 mm is placed over the layup followed by a distributor mesh of about the same size. The distributor mesh helps in resin transport.

There are four most important steps in the VARTM. 1. Mold preparation and fabric lay-up. 2. Sealing the mold and creating a vacuum. 3. Resin preparation. 4. Resin impregnation. 5. Cure of fabricated panels. The solid base used for the fabrication of the CFRP panel is a 6.35 mm thick glass plate. A coating of sand paste wax is applied to the surface for easy release of the composite panel. The top release fabric or peel ply is a porous material fabric which allows for easy removal of the fabricated panel from the distributor medium, connectors and vacuum bagging above. The peel ply sheet is Airtech Bleeder and is cut to dimensions of 482.6 mm x 431.8 mm size. Peel ply is placed on the top of the carbon fiber layup. This helps in easy release of the composite panel after fabrication from the vacuum bagging and supports easy resin flow. The fabric which is unwoven roving IM7 Carbon zero degree is cut to dimensions of 406.4mm x 304.8mm. Sixteen plies of similar dimensions are cut and stacked in the 0-degree direction. The fabric is stored in a room with controlled temperature and dry atmospheric conditions. The distribution medium is

NALTEX green mesh is placed on top of the top release fabric. This assists in maintaining an even distribution of resin on the top of the panel and also assists the flow of resin through the thickness of the panel.

The resin transfer media or distribution media is cut to dimensions of 482.6 mm x 431.8 mm. A PE spiral wired wrap tube of half inch outer diameter was cut to 279.4 mm in length and is used as the resin distribution tube. This tube extends 10mm over the longest edge of the layup. Similar tube of same dimensions is used as the vacuum line. These tubes are laid above the distribution mesh at the two edges along the length of the carbon fiber lay-up. The resin line is connected to resin supply with the help of an airtech three-way connector. The vacuum line is connected to a vacuum pump through the resin trap attached to a vacuum gauge. Nylon bagging film manufactured by Airtech is cut to dimensions of 889 mm x 762 mm, and was used as the vacuum bag. This film is placed over the mold area and was sealed firmly using extruded sealing compound (airtech tacky vacuum sealant). The sealant sealed off the vacuum bag and helped to maintain a uniform vacuum throughout the experiment. A vacuum gage examines the vacuum in the entire vacuum bagged setup during the resin flow process. It also hints any leaks in the bagging. About -25 in Hg of vacuum is pulled to test the bag for any leaks before commencing the resin impregnation process. During the resin impregnation process the vacuum is monitored and maintained at about -25 in Hg. Once the leaks have been removed and the vacuum bag completely sealed, the setup is now ready to be impregnated with the resin. Once the resin is ready, it is injected into the mold. The flow of resin is controlled with the help of a vacuum pump in such a way that it is allowed to flow and this process is continued until the whole panel is soaked in resin. To ensure all layers are properly coated, resin is spread on each layer in a hand layup technique before going through the VARTM process. IM7 continuous unidirectional weave carbon fibers (CST Composites, CA) were used. Once the entire lay-up and all components in the vacuum bag have been wet or impregnated, the resin line is shut off. The vacuum pump is kept on for about 3 hours

to make sure there no more air bubbles in the vacuum bagging. The mold is kept at room temperature for the next 24 hours for green cure. Post-curing is done in an oven set at 121° celsius for 6 hours and 15 minutes. These post curing parameters were implemented according to resin supplier guidelines. The schematic of VARTM and the real-time setup are shown in figures 2.1 and 2.2 respectively.

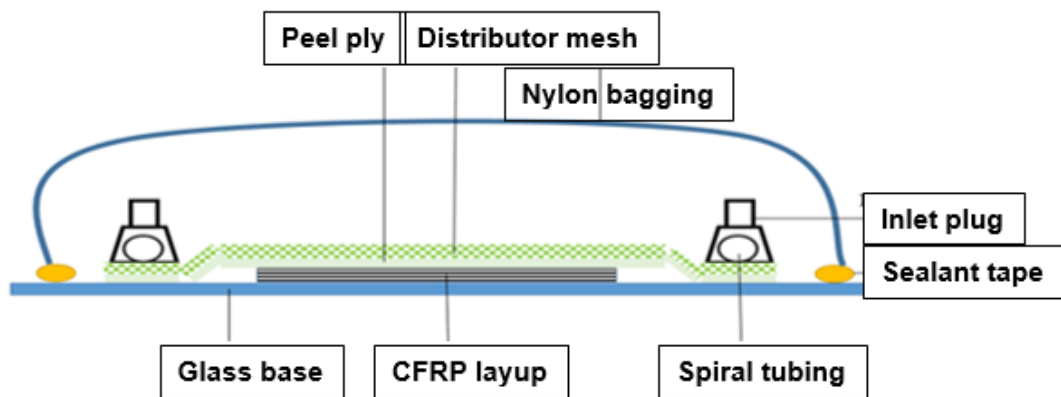


Fig 2.1 Schematic of VARTM setup

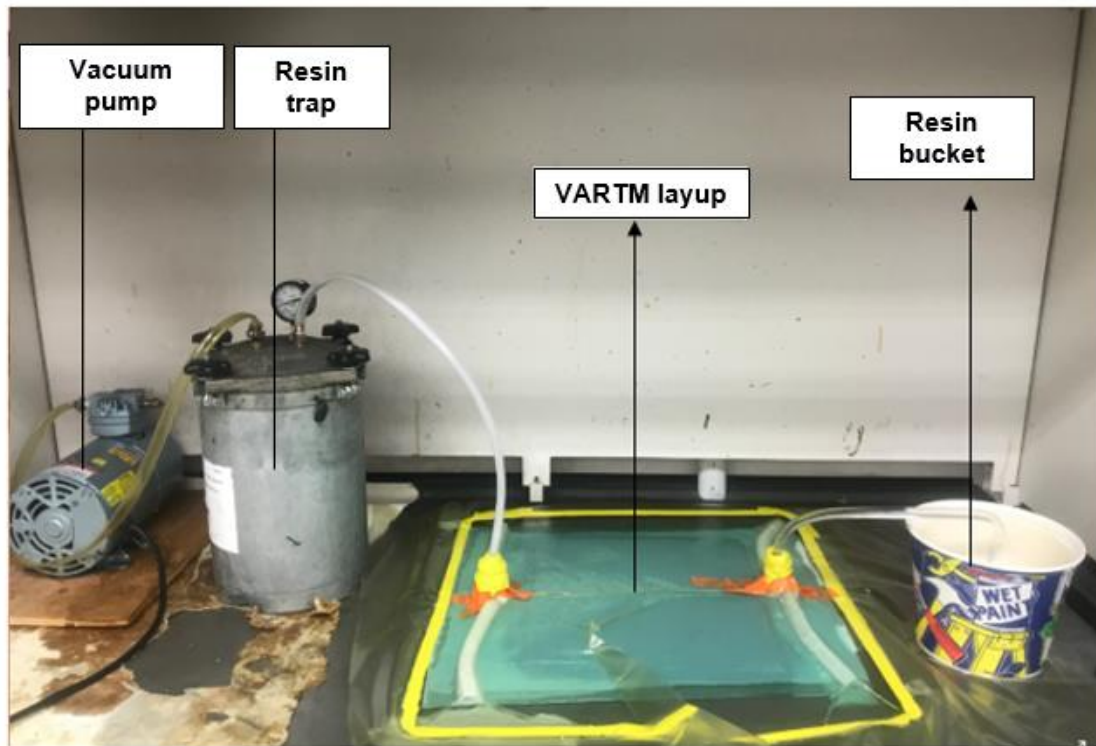


Fig 2.2 VARTM setup under fume-hood

2.3 Experimentation setup for direct current exposure

There are three considerations for the electrical setup that had to be addressed (i) effective constant current application by a high power DC Power supply system with a high power rating, high accuracy and control over set period of time (ii) reliable and repeatable temperature reading and recording device with high accuracy and control over a set period of time (iii) reliable electrode fixture to guarantee an uninterrupted flow of DC through the CFRP sample for any amount of time.

This test setup is based on the accomplishments of Telitchev et al. (2008)[27], Sierakowski et al. (2008)[19], Zantout(2009)[21], and Deierling (2010)[28] who investigated carbon fiber polymer matrix composites subjected to electric currents to test the mechanical response to low velocity impact. The studies emerged from the same evolutionary test setup intended to pass current and subsequently test low velocity impact resistance on CFRP.

Figure 2.3 shows the complete schematic of the electric setup. The HP Agilent 6031 A system power supply, 1000 W was chosen to provide electrical current to the composite specimens. The HP Agilent 6031 A has a current rating of 120 A and a voltage rating of 20 V DC. The 6031A also has a programming accuracy Voltage (at 25° C ±5° C): 0.035% ± 15 mV. Programming accuracy of current (at 25° C ±5° C): 0.2% ± 25 mA. The greatest advantage of the Agilent 6030A is that it can be interfaced to a personal computer with the help of a GP-IB. GPIB cable used in these experiments is 82357B USB/GPIB high speed USB 2.0 interface. 6031 A system is both listener and talker. Upon command, the power supply will measure its output voltage and put the value on the GP-IB. Instructions can be given to the DC power supply system through SCPI command language. I/O path names which are unique to every instrument is communicated to the computer by typing in the I/O path address whenever asked for. This acts as an address identifier by the programming language to identify the corresponding device connected to the personal computer.

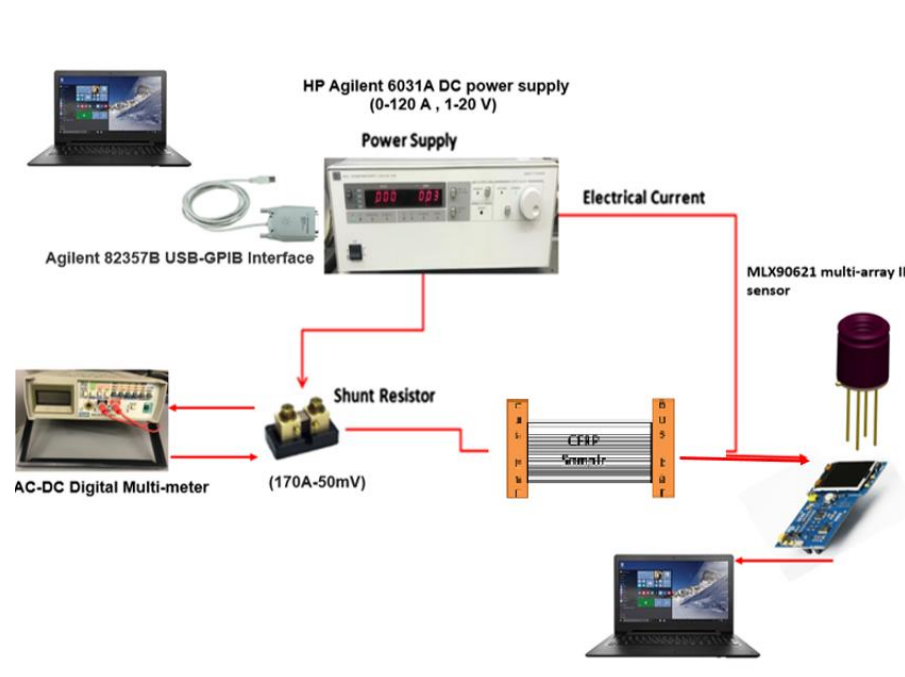
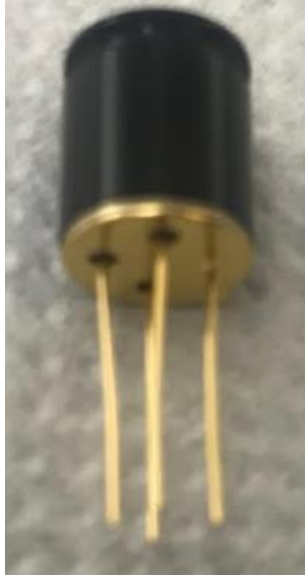


Fig 2.3 Schematic of electric test setup.

A shunt resistor was placed in series with the current application to the composite specimens. The shunt resistor selected was the Deltec MKB-170-50. This shunt resistor has a rating of 50 millivolts (mV) and 170 A, which equates to a resistance of 0.3 milliohms ($m\Omega$). When voltage measurements are taken across the shunt resistor, the current is calculated at any given point in time by dividing the voltage by the shunt resistance of 0.3 $m\Omega$, using Ohm's Law. This has to be reading shown on the DC power supply when the circuit is shorted and the only significant resistance is the shunt. This check serves as a method to validate the output by the DC supply. The digital multimeter (DMM) is used to measure current/voltage across the shunt resistor or across any segment of the circuit with the help of two insulated alligator clips. The reading on the DMM can be cross verified with the DC power supply if the measurements are taken across a shunt resistance with known resistance value and keeping the remaining circuit shorted.

Two personal computers have been used in this test setup in order to record voltage and temperature log files continuously. USB-GPIB interface cable communicates between DC power supply system and computer. A-B USB cable connects computer to the IR sensor breakout circuit. MLX90621 is a far infrared multi array sensor with a high speed to low noise performance. It does high precision non-contact temperature measurements and presents it in a 16 x 4-pixel thermal array. It has a field of view of $30^\circ \times 120^\circ$. It is Factory calibrated in wide temperature range of -40 to 85°C for sensor temperature and -20 to 300°C for object temperature. It comes with high speed I2C digital interface for fast data transfer to the circuit breakout that houses this sensor. Figure 2.4 shows the usage of 4 pins attached to the sensor head. Two pins are responsible for supply and grounding of electric power. The other two pins are data transfer pins. One pin receives and sends signals to the clock within the breakout circuit. The other pin transfers the sensed temperatures as an analog signal.



Pin Name	Function
SCL	Serial clock input for 2 wire communication protocol
SDA	Digital input/output for 2 wire communication protocol
VDD	External supply voltage
VSS	Ground (case)

Fig 2.4 16x4 Melexis multiarray sensor

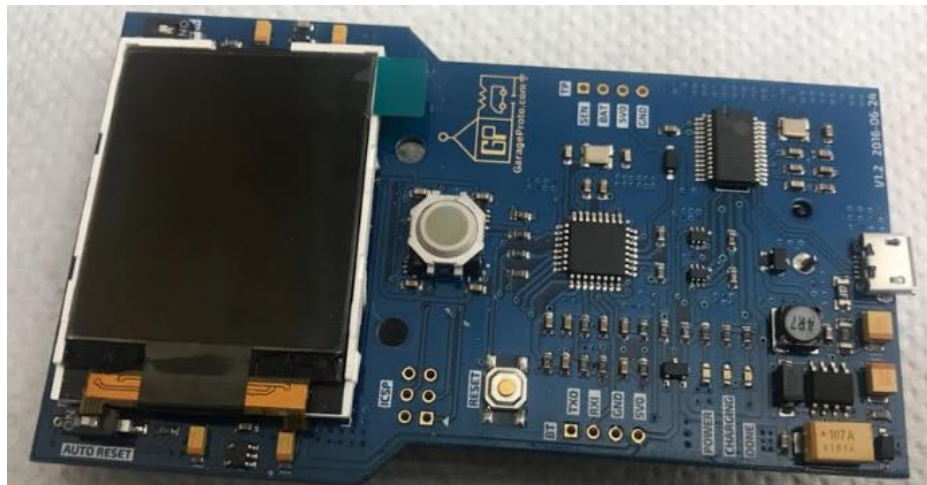


Fig 2.5 Circuit breakout for Infrared imaging

Programming and calibrating the circuit of the breakout as shown in figure 2.5 is an easy task with ICSP connector to either load a new bootloader or program the flash. USB serial converter used to program and view the serial data on computer. The breakout also comes with a Sensor-view display tool which display the 16 x 4-pixel data on computer screen which can be logged into file with .log extension as shown in the figure 2.6.

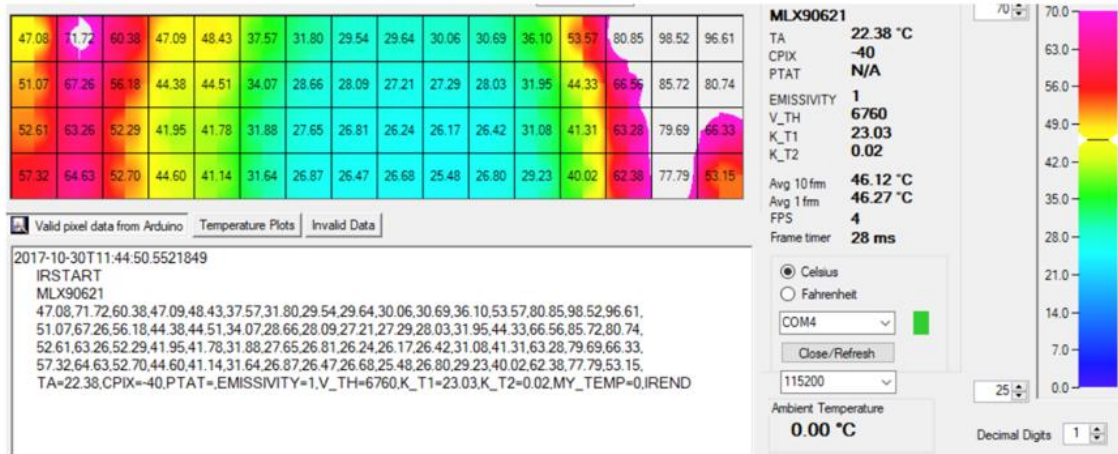


Fig 2.6 Monitor display of thermal pixel information.

This electrical setup is unique in integrating voltage reading and temperature mapping systems in a comparable time scale of recording and storing data. In the previous setups a proper mapping of current flow was not present. Therefore, the growth and decay of current induced temperatures was nonexistent. Presence of a pixelated IR map enables to sense the temperatures for a very small region and compare it with close by regions very easily.

The present electrode test fixture is adapted from Zantout (2009). He designed a custom test fixture to hold CFRP samples to sustain impact loads while passing current pulses. The test fixture needed to (i) be usable as a standalone bench top unit (ii) accommodate 304.8 mm x 177.8 mm CFRP specimen plate of a fixed thickness (iii) provide a foundation for mounting thermocouples or expose an area in middle of the sample to IR scan for temperature measurements.

The parts in the figure mainly are the top and bottom copper electrode plates, fastening screws, screw with electric contact, high temperature spacers and the CFRP sample. Copper electrodes are clamped into contact with the edge of CFRP sample using conducting couple of ¼” screws. Both the plates have about 12 threaded holes side by side to allow clamping at 12 different sites for a variable specimen width. The top surface of the bottom plate is screwed to a 10-gauge copper multi core wire. The foundation over which the fixtures sit is made of steel that can sit on a bench. The part that fits between the bench top base plate and copper electrode base and is fabricated from high temperature ¼” thick insulating polymer. A high temperature insulating polymer thin spacer intended to act as an insulator between copper electrode and bottom surface of the sample is also in place. Figures 2.6 and 2.7 show a schematic and real-time electric fixture setup respectively.

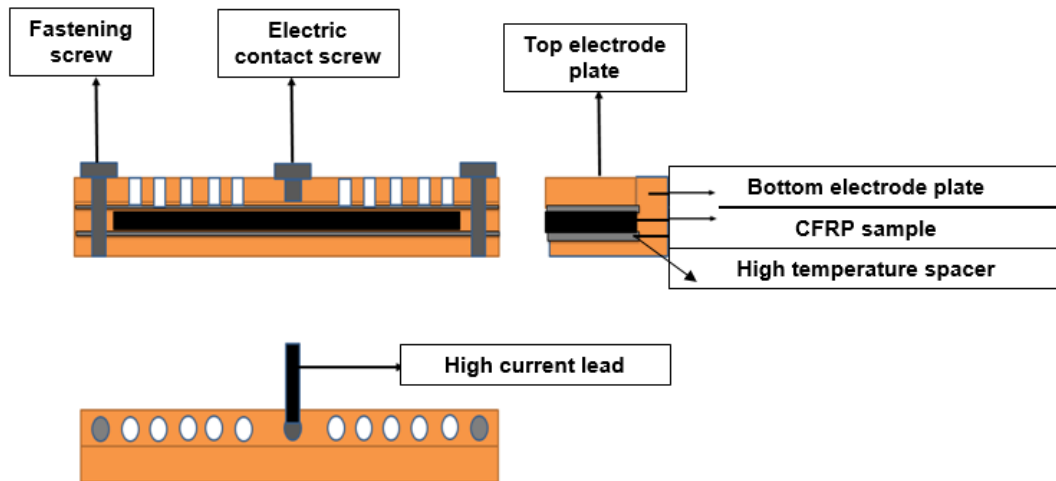


Fig 2.7 Schematic of Electric fixture.



Fig 2.8 Real time electric fixture

Contact heating occurs at the interface between the copper electrodes and the edge surface of the composite specimen. The danger of contact heating is burning of the epoxy matrix at the composite/electrode interface. This acts as an impediment to the intended even current flow along the sample. This heating occurs due to constriction of current at the composite/electrode interface. Surface roughness, surface corrosion, small contact area and dissimilar electrical properties contribute to contact resistance (Braunovic, 2007)[29]. In the case of contact between a copper electrode and a carbon fiber polymer matrix composite, the main influencer of contact resistance is the surface roughness of the CFRP specimens. In these experiments, the surface roughness was developed during the process in which the specimens were cut from a larger plate by a tile cutting saw machine which is not free of vibrations and disturbances. Therefore, contact between the edge of the specimen and the copper electrode is not uniform. This is because of the inherent surface roughness in the specimen due to frayed individual fibers and kind of contact between polymer and fiber. This roughness causes current to constrict and flow through some points rather than the whole edge resulting in contact heating or hot spots.

CFRP also has high surface resistivity. This is the prime reason for bad electric contact between CFRP/metal and CFRP/CFRP. Voltage across the arc struck root thickness is greater for CFRP compared to aluminum and therefore more energy transfer occurs across the interface of a polymer matrix composite. Zantout (2009)[21] and Deierling (2010)[28] applied a thin layer of Duralco 120 silver-filled epoxy to the edges of the CFRP specimens that came in contact with the

electrodes. The reason for applying a layer of electrically conductive epoxy to the composite specimen is to smooth the surface of the composite so that flush contact with the electrode is possible due to increased surface area thereby reducing the contact resistance. This method has been validated by Tudela et al, [30] who investigated electrified composites. In order to obtain consistent electrical results, all samples are prepared using the same procedure.

First, the composite edges are sanded lightly manually using fine grit sandpaper. This was done to remove any imperfections on the contact surface such as rough edges or stray fibers coming out from the contact surface. Next, Duralco 120TM silver-filled epoxy is mixed with resin to hardener in 100:3.5 weight ratio as specified by manufacturer. The epoxy is applied so that all roughness in the contact surface are filled and levelled over with epoxy. Excess epoxy was removed while still wet. Then specimens are then left to cure for 24 hours at room temperature. After the epoxy is cured, the specimens are sanded on the contact edges in the following procedure in order. Firstly, with rough sandpaper 220 grit. Next 320 grit, 400 grit, and 600 grit sandpaper in order are used create almost flat and smooth contact surface.

2.4 Experimentation method

The idea is to expose two size configurations of samples such as 254 x177.8 mm plate and 139.7 x 12.7 mm coupon sized samples to two suitable current intensities which can generate currents high enough but not so high that the polymer matrix starts burning. It has been found through series of trial and error experiments that current intensities of 0.062 A/sq mm and 0.093 A/sq mm as shown in table 2.1 were suitable for coupon and plate samples respectively. These two current intensities generated maximum temperatures above glass transition temperature but not high enough to burn the composite. Post exposure to the current, it has to be confirmed that whatever changes are expected to be seen within the samples, are due to current only but not induced temperature effects. To resolve this issue, the samples were also exposed purely to

temperatures for the same duration for which the samples were exposed to current in an oven. The temperatures selected were the maximum temperatures obtained from current exposure studies. The time durations selected for both the studies are 3 and 6 hours. This could help confirm any changes within the samples influenced by the period of exposure.

Size of sample	Constant Current exposure	Temperature exposure	Duration of exposure
139.7 x 12.7 (Coupon size)	0.062 A/sq mm (2.5 A)	85 deg C	3,6 hours
254 x177.8 (plate size)	0.093 A/sq mm (20 A)	120 deg C	3 hours

Table 2.1 Design of DC exposure experiment

In plate configuration the number of samples tested were approximately 16 samples per plate. Each sample is associated with a particular temperature that developed over a period of time for experimentation. Although there are so many samples that are cut out from the plate, the actual number of samples that truly are exposed to current are very less within the whole plate due to weak conducting contact surface. Those samples are only included in calculating the intensity of current passing through the plate as a whole. The average compression strength, Tg values have only been reported although rest of the samples have also been characterized and evaluated for compression strength and Tg.

In order to exclusively study the effects of currents at a lower sized sample, the coupon tests have been considered. The size is exactly the same size as required for compression tests. The mean and maximum temperatures obtained from IR maps were recorded over regular intervals of time and saved. These temperatures were instrumental to decide how much oven exposure of samples should be done. Coupon sized samples ensured single conduction path and avoided all confusions within the pate sample study.

2.5 Combined Loading Compression Test

LT Drzal et al (1990) [31] have conducted a series of experiments to determine a relation between fiber-matrix adhesion as determined by the single fiber matrix interfacial strength tests with the compressive properties and failure modes of unidirectional carbon fiber polymer composites. Differently surface treated carbon fibers such as no treatment, surface treated and surface treated and coated with thin layer of epoxy were tested for changes in interfacial shear strength. Also compressive tests for strength and modulus were conducted on unidirectional CFRP samples with same kind of corresponding treated fibers and polymer matrix. It has been found that the change in modulus was pretty insignificant while the change in the strength and strain were significant.

Following the above idea, it is worthwhile to conduct 0 degree compressive tests on CFRP samples and compare the change in maximum compressive strengths between as-is and electrically conducted samples. ASTM-D6641 is the standard test method for compressive properties of polymer matrix composite materials. It uses a combined loading compression (CLC) test on all test samples. This test determines the maximum compression strength and stiffness properties of polymer matrix composite materials using CLC test fixture. The specimen is 139.7mm long and 12.7 mm wide having an unsupported length of 12.7mm when installed in the fixture.

Bending and Euler buckling failure modes must be avoided to obtain perfect compression strength values. This can be done by using tabbed top and bottom ends of the fixture as shown in the figure 2.11. The gauge length must be comparable to the length of the specimen such that buckling is avoided in thin specimens. Excessive torque or less than enough torque on the tightening screws of the fixture can prove detrimental to the final compression strength values. The assembled fixture is placed between well-aligned, flat platens (platen surfaces parallel within 0.001'' across the fixture base in the testing machine.



Fig 2.9 Combined Loading Compression (CLC) Test Fixture (ASTM D6641)

The specimen in compression to failure is loaded at a nominal rate of 0.05in./min, while recording force, displacement, and strain data. Load versus strain (or displacement) is recorded continuously or at frequent regular intervals. A sampling rate of 2 to 3 data recordings per second, and a target minimum of 100 data points per test is obtained. The compressive strength of the laminate is calculated using formula $F_{cu} = P_f / w \times h$ where F_{cu} is laminate compressive strength, MPa, P_f is maximum load to failure is in N, w = specimen gage width, mm, and h = specimen gage thickness, mm.

2.6 Digital Scanning Calorimetry

Glass transition temperature is a temperature range within which a thermosetting polymer changes from rigid glassy state to a more flexible rubbery state. It is a temperature range over which the mobility of the polymers increases significantly[31]. T_g is determined by factors such as

chemical structure of epoxy resin, type of hardener and degree of cure[32][33]. In our case, all these factors are kept constant and the only change if observed could be because of the direct currents passing through the polymer. Tg invariably acts as an indicator to some mechanical properties of the polymers. Higher the Tg higher the crosslinking density and higher the strength. Same is true with lower Tg. A higher Tg along with a higher storage modulus which results in a high stiffness which in most cases relates to a low percent elongation and poor energy dissipation when stressed. Comparing glass transition temperatures (Tg) of as-is and electrically conducted CFRP samples is very crucial in finding the influence of intensity and duration of DC currents on the crosslinking response of the epoxy resin matrix within the CFRP sample.

Tg is usually measured using Differential Scanning Calorimetry standard ASTM E1356. Q2000 differential scanning calorimeter manufactured by TA Instruments, New Castle, DE, USA is used to perform DSC measurements. The heating rate is 10⁰/min. This apparatus works on the principle of comparing change in heat capacities of incoming sample placed in lid and pan arrangement with empty lid and pan reference. Weights of T-zero lid and T-zero pan were measured using a precision scale. A small portion of sample of about 10 mg[34] weight is taken and placed in the pan. The lid is placed on top of the pan and pressed hard to lock the sample. The ready sample is then kept in auto sampler slot and the slot number is recorded. A reference lid and pan is weighed and pressed together. It is then placed in one of the remaining auto sampler slots and its number is recorded. The software of the apparatus provides allows to perform tests in a sequence. Each sample weight and its lid-pan weight are given as input along with auto sampler slot number corresponding to the sample. In the first cycle, sample was equilibrated to -15 °C and then subjected to isothermal conditioning for one minute. Temperature is then ramped up to 150 °C at a rate of 10 °C/min and again sample was allowed to undergo isothermal process for one minute. It is done to erase previous thermal history of the sample. Cycle two involved reducing temperature to -15 °C at a rate of 10 °C/min followed by isothermal process for one-minute duration. In cycle three, temperature of

sample was increased to 150 °C at a rate of 10 °C/min and then it was subjected to isothermal process for one-minute time span. After all samples are tested, heat flow – temperature plot is obtained to depict thermal history of the sample. The third cycle is used to obtain T_g as specified at the beginning of the test.

2.7 Density and Fiber Volume Fraction

Fiber fraction experiments were performed according to ASTM D3171. A 70% nitric acid was used for the matrix digestion. Small rectangles approximately 0.3-0.5 grams were cut with a hacksaw from tested CFRP samples. Three samples were weighed to the nearest .0001 grams. The method employed for the matrix digestion was microwave digestion. Three of the samples of each category of exposure underwent microwave digestion where each was placed in a special bomb with 3 ml of acid and microwaved for 1.5 minutes in a fume hood. They were allowed to cool and were washed three times with cool water then with methanol and placed in a curing oven to dry at 100° C for 1 hour. The fiber remnants were again weighed and fiber weight fraction was calculated by $W_r = M_i/M_f \times 100$ where $M_{i,f}$ is the respective initial and final masses. Void fraction is also calculated likewise.

This density test method is for determination of the density of polymer composites in forms such as CFRP. The ASTM standard is D792 is followed for this procedure. Density done for a number of samples is basically helpful in determining the changes within a sample exposed to different test conditions, uniformity across the samples and as a representative for a huge sample space. Samples may differ in density due to their differences in porosity and composition.

Sartorius™ density determination kit is used to determine the density of all the CFRP samples. The Archimedeian principle is used to determine the density of solid using this machine. As the samples are expected to have density above 1 gm/cc (as they don't float on water) the method for determining density is different compared to that of the other densities which are

equal or less than 1gm/cc. Determination of density is a very simple process and involves only four steps. In the first step a small sample of small size which is around 1-5 gms is cut from the representative area of the CFRP. In the second step the weight of the sample is measured in the sample air. Then the buoyancy force which is difference of the sample weight in the air and in the water is calculated directly from the instrument. It is a negative value. Then the density or specific gravity of the solid is measured using the formula:

$$\rho = [W(a) \cdot [\rho(fl) - 0.0012 \text{ g/cm}^3] / 0.99983 G + 0.0012 \text{ g/cm}^3]$$

$W(a)$ and G are measured in gms, $\rho(fl)$ is measured in gm/cm^3 , $G = W(a) - W(fl)$

CHAPTER III

RESULTS AND DISCUSSION

3.1 Voltage history profile

CFRP samples of different sizes such as 254 x177.8 mm plate and 139.7 x 12.7 mm compression test sized samples are subjected current intensities of 0.093 A/sq mm and 0.062 A/sq mm respectively. The intensity of current passed was restricted based on the expectation of temperature that could possibly develop on the sample surface. Higher surface temperatures although not close to the vaporization temperatures of polymer matrix, the possibility of hot spot generation and its interruption to current flow is more and more evident. The current conduction has been performed under constant current mode. Based on ohms' law when the current flow is constant, the variable that can change are resistance and voltage. The DC power supply measured the change in the voltage which is a direct indicator of change in the resistance. The internal change happening within the sample due to exposure of direct currents of different intensities and durations is evident in the resistance change and change in the temperature mapped over the mid-span of the samples.

The fiber volume for both plate and coupon sized samples was around 56% and 55% respectively with void percentage around 6-8 % and 7-9 % respectively. Although this is quite inferior compared to the commercial CFRP, these can still be used for comparative studies. The densities obtained were around 1.4-1.5 gm/cc for all sample representatives

Figures 3.1 and 3.2 show the voltage history plots for five 139.7 x 12.7 mm sized samples for 3 hours and 6 hours current conductions each. The constant direct current passing through them was 2.5A which is about 0.062 A/sq mm intensity of current. For voltage history in figure 3.1 five samples have been subjected to constant current conduction along the fiber axis. A standard mean and mean deviation was not possible to calculate for these samples because of different nature of curves exhibited by every sample. Two different phenomenon are associated to this inconsistent

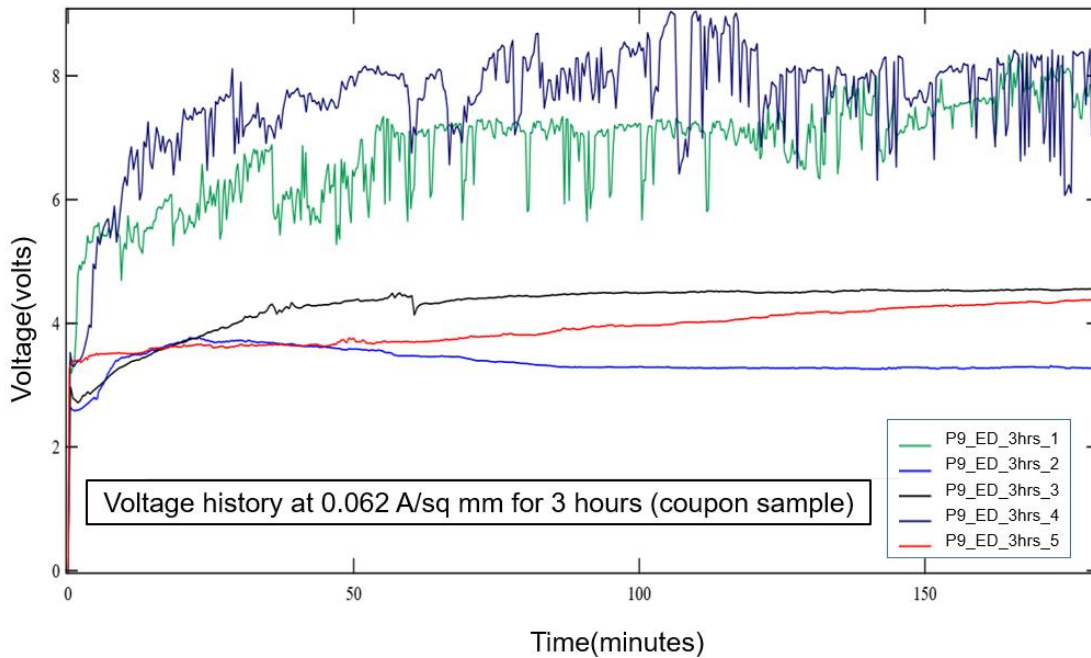


Fig 3.1 Voltage history for 3 hours at constant current: 0.062A/sq mm

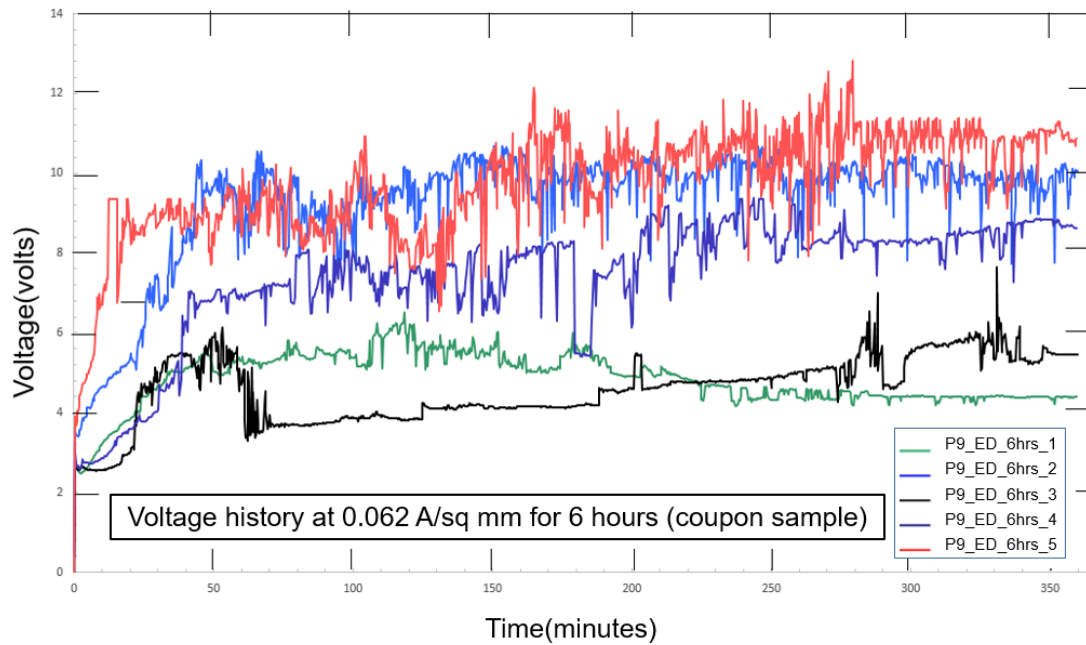


Fig 3.2 Voltage history for 6 hours at constant current: 0.062A/sq mm

and erratic voltage history behaviors. The hot spot formation at the electrode and sample interface causes burning of the epoxy in the local current inlet areas. This has a very straightforward effect on the fluctuation within the resistance of the overall circuit. If the hot spot formation and localized burning of the epoxy does not subside within the conduction period, the plot has a range of disturbance in the order of 2 volts. The hot spot formation is also supported by the temperature plots obtained for samples P9_ED_3hrs_1 and P9_ED_3hrs_4 whose temperatures are higher compared to the rest of the samples. Also, the end cross section of the samples shows a burnt epoxy layer at the tip in case of hot spot formation. This could be observed in the case of sample P9_ED_3hrs_4 and P9_ED_3hrs_1. However, the overall trend for complete 3 hours shows a steady increase in the resistance from 6V to 8 V in case of sample P9_ED_3hrs_4. This is similar with sample P9_ED_3hrs_1 whose resistance increased from 5V to 8V. Samples P9_ED_3hrs_3 and P9_ED_3hrs_5 show a similar trend in their voltage history. They show a very low rate of

increase in resistance. The increase in each of the sample's resistance is not more than 1V. Sample P9_ED_3hrs_2 shows a different trend where the overall resistance drops from 4 V to 3.2 V.

The overall increase in the resistance is attributed to the fact that the carbon fibers have a negative coefficient of thermal expansion. This can cause little loosening of the sample between the electrodes during the passage of current. Along with this claim, the other reason could be the increased random free movement of the epoxy molecules in the vicinity of the fiber due to influx of electric energy through flowing charges and associated thermal energy induced. These random motions of epoxy molecules can hinder the effective conduction capability of the carbon fibers however insignificant. Figure 3.2 shows voltage history for 6 hours on same afore-mentioned sample sizes. Samples P9_ED_6hrs_2, P9_ED_6hrs_4 and P9_ED_6hrs_5 show a similar trend as that of samples P9_ED_6hrs_2 and P9_ED_6hrs_4 in figure 3.1. There is an overall increase in the resistance from 9 V to 11 V. One might expect the voltage history plots to be same for both figures 3.1 and 3.2 at least till 180-minute mark, which is rarely a possibility. The initial configuration of sample placement within the electrodes, the internal anisotropy and variation of conduction paths between sample to sample impose a great variation within the voltage history plots which include the initial resistance, final resistance, rate of increase and overall fluctuations due to hot spots formed. Samples P9_ED_6hrs_1 and P9_ED_6hrs_3 have shown lesser fluctuations compared to rest of the samples. Sample P9_ED_6hrs_3 has shown rise in the resistance from 4 V to 6 V after an initial big disturbance. P9_ED_6hrs_1 has shown a steady fall in the resistance from 6V to 4 V. The fall in resistance was observed only twice within ten samples tested. This reduction in the resistance can be attributed to the opening of the new conduction paths within the sample and thereby increasing the net conduction even though the loss of conduction due to negative CTE of carbon fibers and random movement of epoxy molecules act as counterbalances. It can be well observed from both the graphs that, there is no major shift in the nature of the voltage history curve post to 180 mins till the end of the experiment.

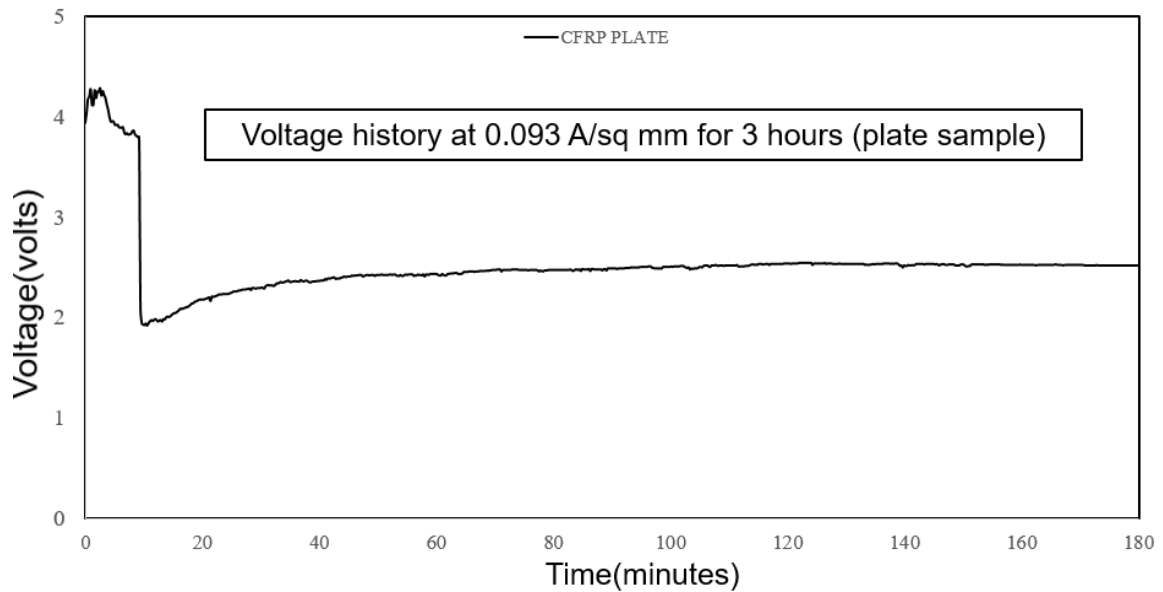


Fig 3.3 Voltage history for 3 hours at constant current: 0.093A/sq mm

Figure 3.3 shows the voltage history for constant direct current conduction of 0.093A/sq mm on a CFRP sample plate of dimensions (254 x177.8 mm) for a time duration of 3 hours. The current intensity equates to 0.093 A/sq mm. This sample size is relatively very large compared to the previous sample sizes mentioned above. The voltage trend observed clearly shows that increase in the resistance is very minimum and very slow compared to smaller samples. The voltage curve almost plateaued at the end of the experiment. The voltage increase was merely from 2 V to 2.5 V which is the most minimum of all samples tested. This is can be purely attributed to the size of the sample-electrode interface. The interface being bigger the total number of conduction paths independent of each other are more possible. This makes the conduction easy through the plate. For this particular plate it has been observed in the IR imaging that there are two conduction paths. The waviness as observed in the previous samples is very minimal in this case. This is because the minor hotspot formations at few local points on the electrode sample interface are not significant enough to trouble the strong conduction paths already established within the sample.

3.2 Temperature history profile

CFRP samples of different sizes such as 254 x 177.8 mm plate and 139.7 x 12.7 mm compression test sized samples are subjected to current intensities of 0.093A/sq inch and 0.062 A/sq inch respectively.

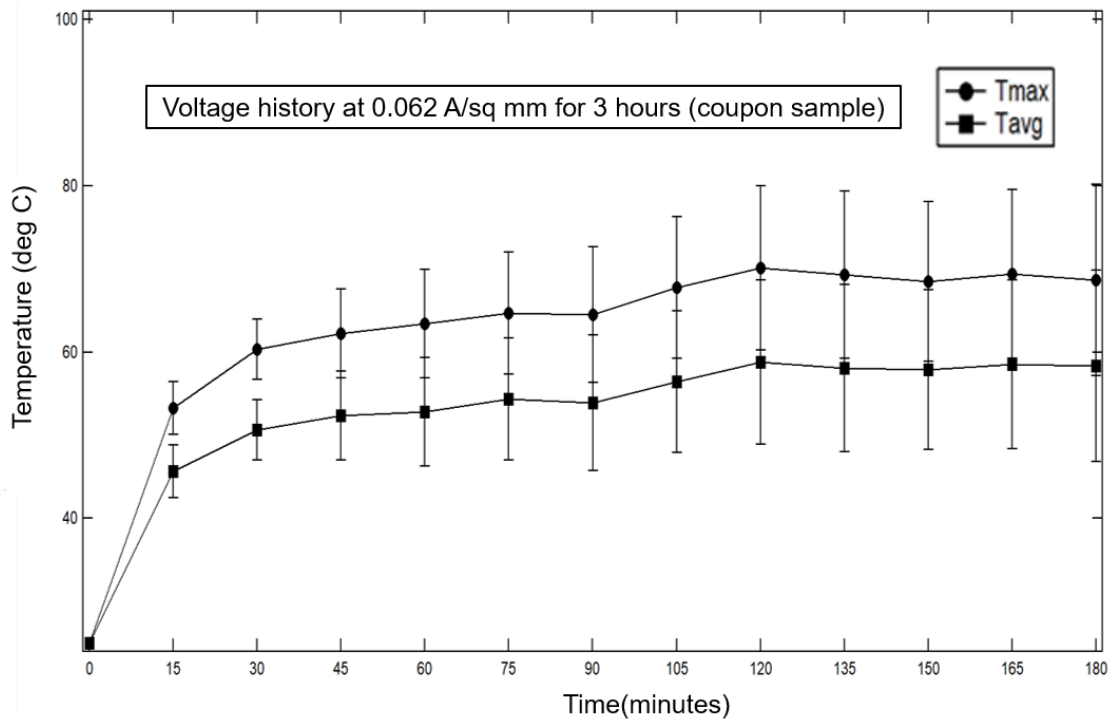


Fig 3.4 Temperature history for 3 hours at constant current: 0.062A/sq mm

Figure 3.4 shows temperature history of five 139.7 x 12.7 mm sized samples conducting 0.062A/sq mm constant direct of current through them. Time duration for passage of current is 3 hours. Temperature developed is not only an indirect identification of the conduction path on the sample, but also helpful in the measuring the range and rate at which the induced temperature due to joule effect is developed over the surface of the CFRP sample. In the figure 3.4, temperature recordings at the mid span of the sample made at every 15-minute interval are plotted. Every sample experiences an average temperature which is the mean of two center pixels on the IR map and

maximum temperature which is the highest of all the four pixels on IR map within a given measuring column. Therefore, we end up with two plots Tavg and Tmax plotted over 3 hours of experimentation. For example, in the box given below the T avg would be average of values 64 and 68 while the maximum temperature would be 69.

x	x	x	x	x	x	x	65	x	x	x	x	x	x	x	x
x	x	x	x	x	x	x	64	x	x	x	x	x	x	x	x
x	x	x	x	x	x	x	68	x	x	x	x	x	x	x	x
x	x	x	x	x	x	x	69	x	x	x	x	x	x	x	x

Fig 3.5 Schematic of temperature multiarray (16 x 4 pixel)

It is quite obvious from the graph that the temperature developed by a single conduction path carrying 0.062A/sq mm current has a steady increase of temperature developed on its surface. The nature and rate of increase of current is similar for both Tavg and Tmax plots with an average offset of 10 °C between. The slow and steady state of increase in the temperature for a sample can be attributed to the fact that the heat developed is not equally dissipated from the sample at the same rate. Therefore, the sample is acting as a heat sink. The other reason for temperature rise is due to the heat conducted constantly from any hotspot that is burnt and therefore acts as a local heat source. The overall temperature rise is from room temperature which is 25°C to a maximum of 69 °C and an average of 59 °C over a period of 3 hours for 0.062A/sq mm of direct current conduction.

Figure 3.6 shows temperature history of five 139.7 x 12.7 mm sized samples conducting 0.062A/sq mm constant direct of current through them. Time duration for passage of current is 6 hours. This plot as expected behaves very much like plot 3.4 till 180 min mark. However, figure 3.4 looked like the temperatures on the sample surfaces are plateaued which is not the case after 180 minute' mark. Till 360-minute mark or till the end of the experiment, the temperature over the surface of the specimens increased more or less in a linear fashion. The offset between Average

temperature and Maximum temperature remained constant throughout the current conduction process. The difference was about 10 °C.

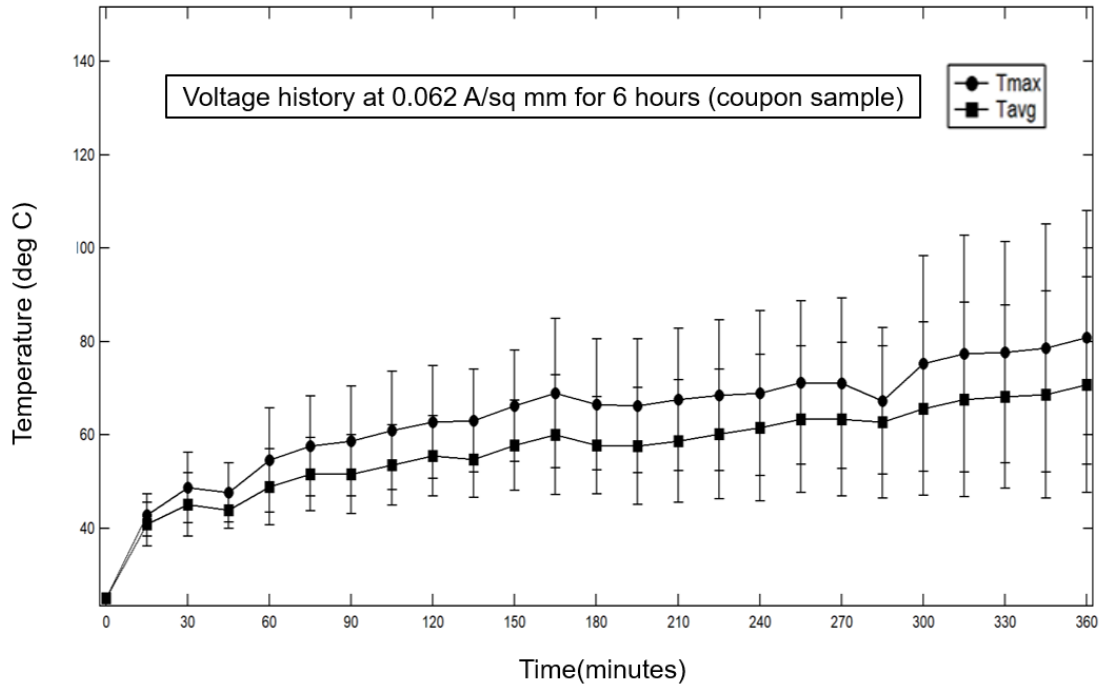


Fig 3.6 Temperature history for 6 hours at constant current: 0.062 A/sq mm

The overall temperature rose from 25 °C to 80 °C for a maximum temperature and 70 °C for an average temperature. It must be noted that the temperature rise in first 180-minute mark was close to 0.11°C/min but the in the second half of the experiment the rise is slow which is just about 0.22°C /min. This can be attributed to the fact that CFRP is acting as a heat sink and the hot spots are definitely conducting heat to mid-span of the sample surface.

The temperature curves for individual coupon samples exposed to 0.062A/sq mm for both 3 and 6 hours have been reported in figures 3.7, 3.8, 3.9and 3.10. The average and maximum temperature values of each sample has been reported separately over time. It is interesting to find that the maximum temperature curves and voltage curves for same sample match in their growth trend.

This validates the argument that the hotspot formation as shown by the fluctuations in voltage of P9_ED_3hrs_1 and P9_ED_3hrs_4 is also seen in increased average and maximum temperature plots of same samples. Similarly, P9_ED_6hrs_5 and P9_ED_6hrs_2 samples exposed to 0.062A.sqmm for 6 hours also shows high voltage values with fluctuation followed by a similar increase trend in the temperature buildup. This observation strengthens the claim that hotspots are a major issue while passing current not only in causing constricted current flow but also influencing the overall temperature growth within a current exposed CFRP sample.

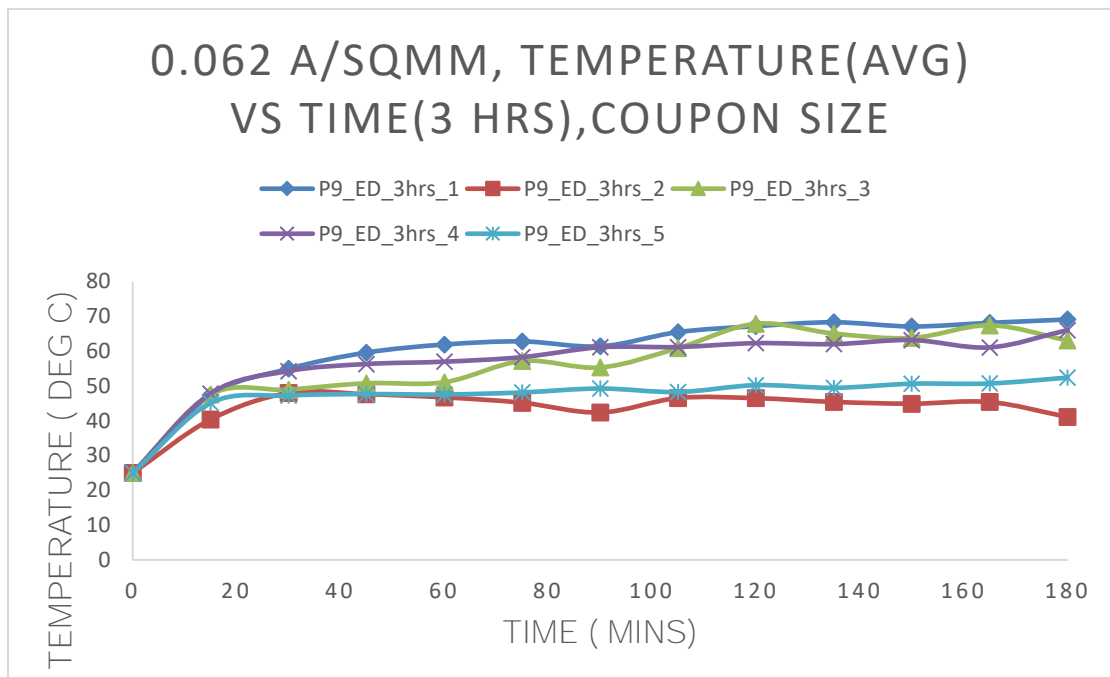


Fig 3.7 0.062 A/sqmm, Temperature(avg) vs time (3 hrs), coupon size

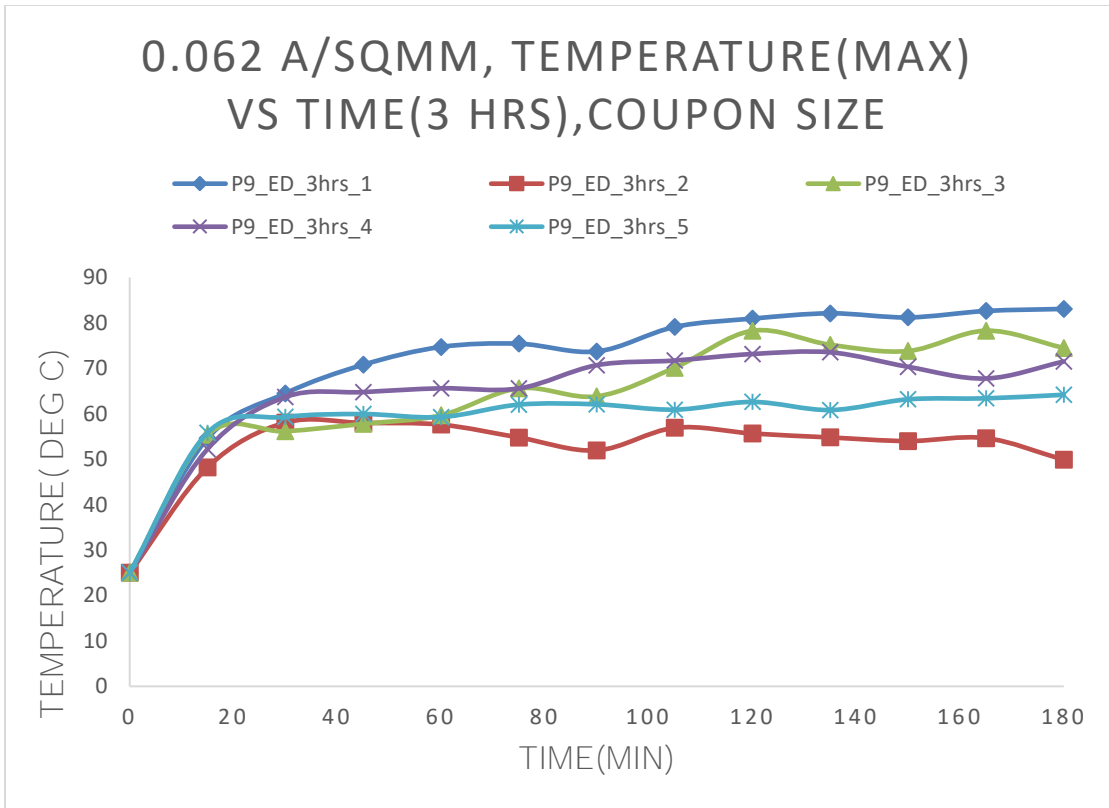


Fig 3.8 0.062 A/sqmm, Temperature(max) vs time (3 hrs), coupon size

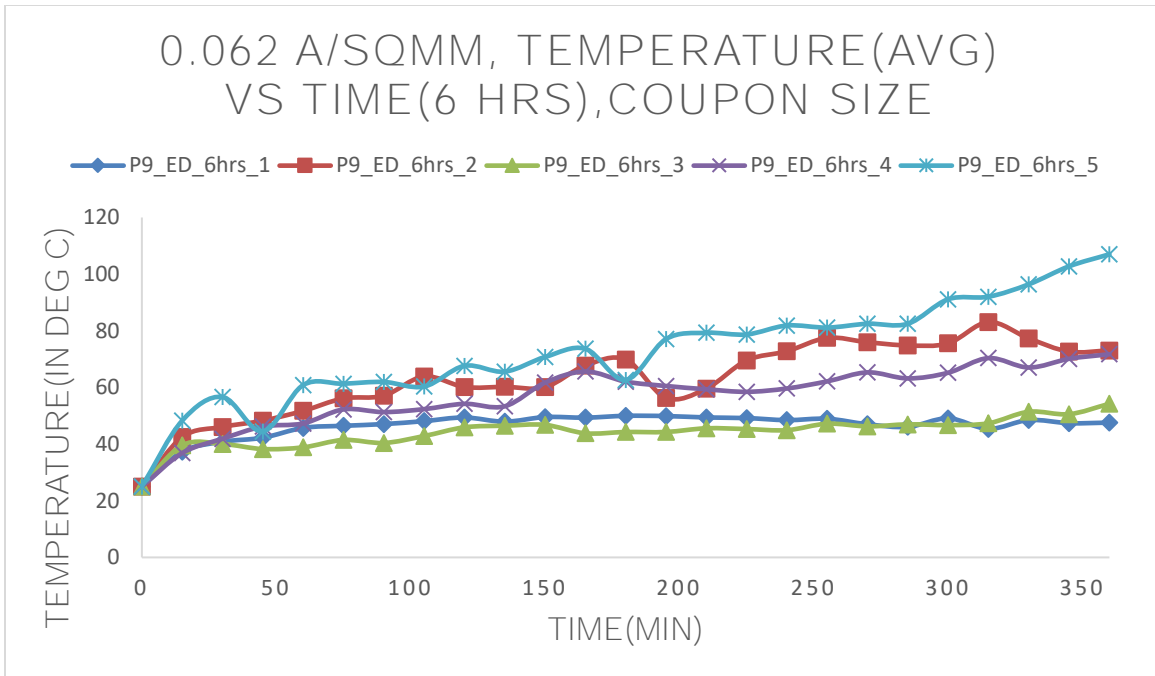


Fig 3.9 0.062 A/sqmm, Temperature(avg) vs time (6 hrs), coupon size

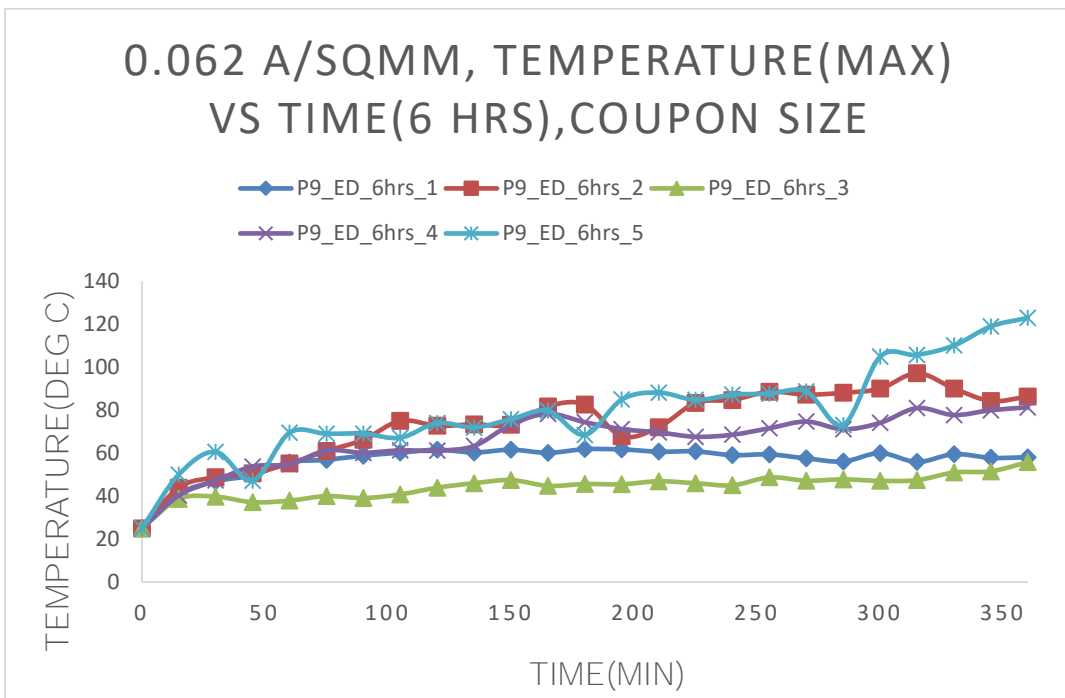


Fig 3.10 0.062 A/sqmm, Temperature(max) vs time (6 hrs), coupon size

Figure 3.10 shows temperature history of sixteen 254 x177.8 mm plate sized sample conducting 0.093 A constant direct of current through them. Time duration for passage of current is 3 hours. The temperatures plotted in the figure are the surface temperatures over the mid-span of sixteen locations all along the mid span width of the sample plate. These temperatures have been recorded every 15 minutes till the end of the experiment. It is important here to mention that there are two identified conduction paths within the sample CFRP plate in this case. Therefore, even when the current intensity is higher compared to previous experiment, the temperatures developed are lower and touch a maximum of 60 degrees at the end.

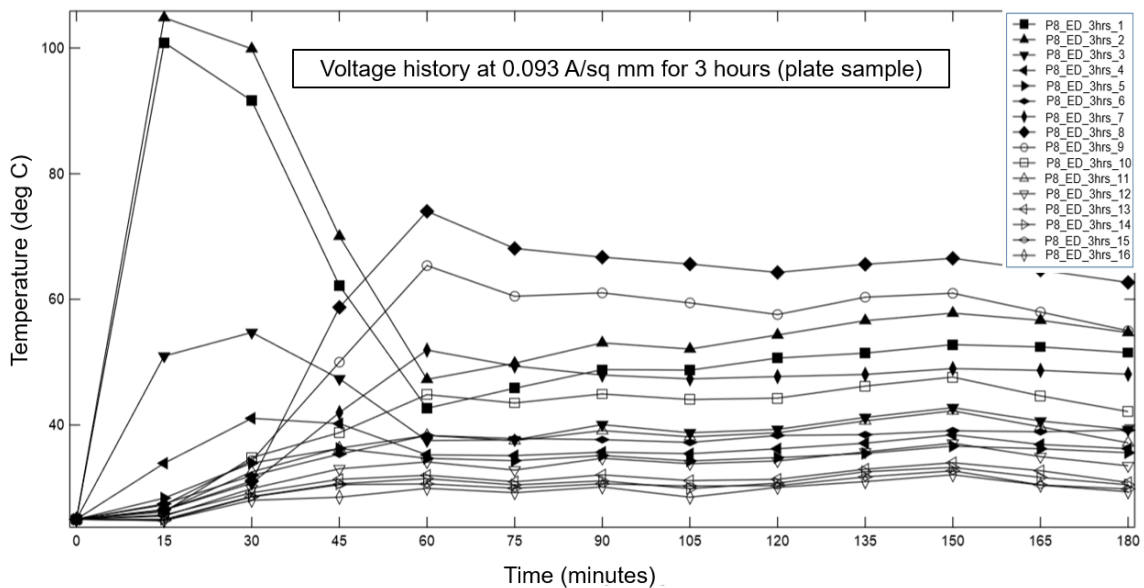


Fig 3.11 Temperature history for 3 hours at constant current: 0.093 A/sq mm

It has to be noted that the initial rise of temperatures over all the samples is very erratic compared to the previous case. It almost took 50 minutes for all the samples to stabilize in their temperatures. This is attributed to the fact that before the 50-minute mark the heats induced by different conduction paths were very much independent of each other while after 50-minute mark they started to interact with each other. Heat conduction became very evident. It can be observed that P8_ED_3hrs_1 and P8_ED_3hrs_2 experienced the first conduction paths and therefore

showed a very high temperature. All the current was flowing through this one channel causing exorbitant rise in the temperatures initially. However, a new conduction path came into existence at samples P8_ED_3hrs_8 and P8_ED_3hrs_9 at 30-minute mark. This created an alternate channel for current to pass and therefore the temperatures over this area increased and stabilized later on. They showed consistently that they carried the highest charge possible as their temperatures were never less than 60 °C as compared to other samples. Samples P8_ED_3hrs_1 and P8_ED_3hrs_2 even though showed a promising conduction path initially gave away for an alternate conduction path reducing itself to second highest channel in passing the current. There is a conduction process that is very much possible within the sample plate and heating profile over a plate from left to right changes over a period of time.

Figure 3.11 is a temperature gradient surface graph recorded for 3 hours. It has sample numbers on X axis which starts from 1 and ends with 16. Samples 1 and 16 are located at two ends of the CFRP plate.

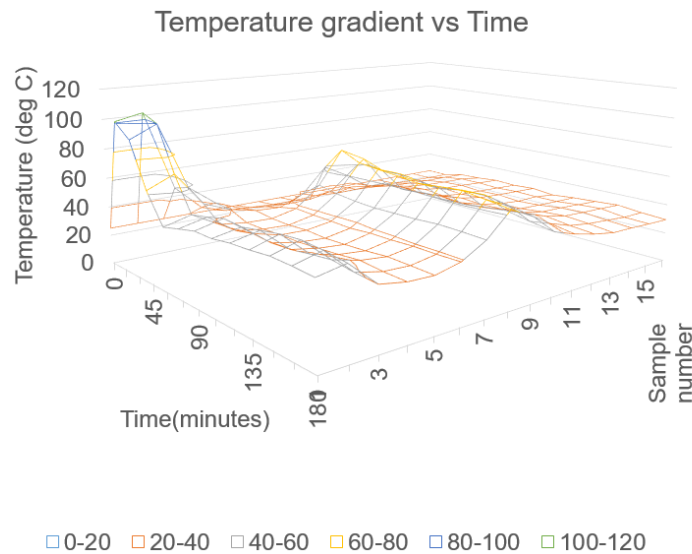


Fig 3.12 Temperature gradient for 3 hours @ constant current: 0.093A/sq mm

It can be clearly observed that samples 1 and 2 experienced high rise in temperature early in the experiment but dropped very soon and continued to have a lower temperature profile compared to

all other samples. This is clearly because after high conduction and rise of temperatures above 80 °C these conduction paths almost became inactive due to hot spots that may have possibly formed acting as barriers for current conduction. The maximum sustainable temperature for a continued conduction was slightly less than 70 °C. It is interesting to note that this temperature is close to the glass transition temperature of this polymer matrix.

3.3 Maximum Compression Strength

Maximum compression strength test as shown in table 3.1 was performed on 5 samples each for every category of exposure which includes exposure to current passage of 0.062 A/sq mm for 3 and 6 hours and oven heated samples at 85 °C for 3 and 6 hours. The intention is to compare the magnitudes of maximum compression strengths for current conducted samples for 3,6 hours, oven temperature treated samples for 3,6 hours with the strengths of as-is samples. Sample size is in accordance with the ASTM standards. It can be observed from table 3.1 that there is no conclusion that can be made over the exact influence of electric current on the CFRP samples. The difference between the as-is samples and current exposed samples for 3 hours and 6 hours show both decrease

Type of sample	Maximum compression strength (Mpa)	Standard deviation (Mpa)
As-is (coupon size)	317.3	30.13
0.062 A/sq mm exposure for 3 hours (coupon samples)	305.8	54.2
0.062 A/sq mm exposure for 6 hours (coupon samples)	326.8	51.0
Temperature exposure for 3 hours at 85° (coupon samples)	302.1	44.9
Temperature exposure for 6 hours at 85° (coupon samples)	323.9	26.4

Table 3.1 Maximum compression strength for 3,6 hours at constant current: 0.062 A/sq mm

and an increase of 3% which is very negligible and difficult to rely on. This is due to the natural inherent deviations from sample to sample are generally very high in CFRP samples. Oven heated samples were tested just to make sure that a remote possibility of curing beyond post curing is not playing an important effect in deciding the post exposure scenario of conducted samples. Clearly we can notice no change even within the temperature treated samples at 85 °C for 3 hours and 6 hours. Not even a marginal 3% difference was observed within the means of 6-hour conduction, temperature treated experiments. Table 3.2 shows a graph plotted for compression strengths of samples cut from electrically conducted samples of size 254mm x 177.8mm. There are two categories of sample exposure which include electrical conduction of 0.092A/sq mm for 3 hours and oven heated samples till 120 °C

Type of sample	Maximum compression strength (Mpa)	Standard deviation (Mpa)
As-is (coupon size)	317.3	30.13
0.093 A/sq mm exposure for 3 hours (coupon samples)	326.8	54.0
Temperature exposure for 3 hours at 120° (coupon samples)	323.9	26.4

Table 3.2 Maximum compression strength for 3 hours at constant current: 0.093 A/sq mm

for 3 hours. The strengths of the exposed samples are compared against each other while being compared to the strength of the as is sample. It can be clearly understood from the graph that the maximum compression strengths of all categories doesn't seem to have a significant difference. The temperature treated sample saw a fall of mere 5% compared to the as-is samples. This is interesting since, a similar trend was observed in the previous experiment where the temperature treated sample fell in the compression strength however small when samples are exposed below 3

hours. However, for the samples exposed for 6 hours there is a slight increase in the strength. The reason behind this is yet to be studied.

3.4 Glass Transition Temperature

Glass transition temperature (T_g) range for a thermosetting polymer indicates the transition from rigid state to more 'rubbery' state. Degree of curing impacts the glass transition temperature of neat epoxy resin [35]. It is therefore understood that the nature of exposure to CFRP samples may have a unique effect on the degree of crosslinking of the polymer matrix. Higher T_g values in epoxy indicates higher degree of cross-linking and better compressive properties at high temperatures. Differential scanning calorimetry is used to easily determine glass transition temperature (T_g) of different samples exposed to a variety of exposure conditions. Q2000 differential scanning calorimeter used in this study has precision of ± 0.01 °C in the measurement of temperature. Mean value of glass transition temperature range are obtained by using two tangents on flat slopes of the third cycle for which thermal history was known. DSC was carried on samples that include as-is, electrically exposed for both intensities of 0.062A/square inch and 0.093 A/square inch for 3 and 6-hour exposure as well as temperature treated samples at 85 °C and 121 °C for 3 hours and 6-hour exposure. Table 3.3 shows the T_g comparison against all kinds of exposure for current, time and temperature. The values for as-is CFRP and net epoxy are also tabulated. Each case of as-is and exposure has three samples tested and the average value to the nearest one decimal has been reported. The T_g values of different current, temperature exposed samples compared to as-is coupon did not vary significantly. Both the values are found to overlap within each other's scatter range. However, the exposure to current intensity of 0.062A/sq mm for 3 hours and 6 hours has a 4°C and 2°C increase in the T_g values respectively. The temperature exposure at 85°C for 3 and 6 hours also has an increase of 5°C and less than one-degree increase respectively. Overall it is understood that the increase in cross linking is better when the sample is heated for shorter periods of time either in the oven or due to current induced heating when the

surface temperature is 85°C. The increase in cross linking is very less when heating is prolonged over 3 hours. The curing of uncured leftovers within the epoxy could be the reason behind changed level of crosslinking.

Type of sample	Tg range (°C)
As-is (coupon size)	47.3
0.062 A/sq mm exposure for 3 hours (coupon samples)	51.4
0.062 A/sq mm exposure for 6 hours (coupon samples)	49.7
Temperature exposure for 3 hours at 85° (coupon samples)	52.3
Temperature exposure for 6 hours at 85° (coupon samples)	47.6
As-is (plate sample)	45.8
0.093 A/sq mm exposure for 3 hours (plate sample)	44.3
Temperature exposure for 3 hours at 120° (plate sample)	44.6

Table 3.3 Tg comparison for all exposures

The Tg values of different current, temperature exposed samples compared to as-is plate sized samples did not vary significantly. Both the values are found to overlap within each other's scatter range. However, the Tg values of polymer exposed to higher intensity such as 0.093A/sq mm and oven exposed at 120°C tend to decrease by one degree compared to as-is samples. This can be attributed to the thermal degradation of the polymer due to high temperatures.

CHAPTER IV

CONCLUSION

The primary goal of this investigation was to identify any change in the quasi-static mechanical response such as maximum compression strength of carbon fiber reinforced polymer exposed to low constant direct currents for relatively longer time durations as opposed to the previous studies. To realize this goal, an experimental electric conduction setup for passing current through 16 layered unidirectional composite plate was developed. This setup included specially designed electrodes, DC power supply/recording system to pass intended constant current for a fixed time and record the change in the voltage simultaneously. The setup also includes Infrared imaging/recording system to map the current stream within the sample in real time. CFRP samples with two different size configurations of coupon and plate are exposed to 40 and 60 A /square inch respectively for 3 and 6 hours constantly while the voltage and temperature readings are taken simultaneously. It is to be noted that the fiber volume fraction for both plate and coupon samples is not varying considerably and therefore we did not see much change in their voltage values.

It has been observed in the voltage history plot that there is a steady but very slow increase within the in the resistance of majority of CFRP samples either coupon size or plate sized for all intensities of current exposure at all times. The resistance increase amounted to 3 % in coupon sized samples to 2% .in plate sized samples. Significant number of samples experienced high fluctuation within the voltage readings. This is attributed to the hotspot formation at the interface between electrode and the sample which plays a significant role in determining the overall resistance

measured across the circuit. The steady increase in the voltage or resistance is the reason behind the steady rise in temperatures within the CFRP samples.

It has been observed in the temperature history plots for coupon sized and plate sized samples are very different. Temperature rise is steady and very slow for both durations of exposure in coupon sized samples. The increase in temperature is due to the fact that CFRP is a heat sink. Rapid heating sometimes is due to hot spot formation at the electrode sample interface. The temperature gradient plot in case of plate sized samples plotted for different times shows a very erratic temperature behavior in the plate size sample. This is because of the multiple conduction paths formed within the sample. Initially the current tries to establish a conduction path through a less resistive path within the entire sample. In these attempts one to many conduction paths originate and die. As a result, multiple places across the width of the sample instantaneously heat up and then conduct the heat into other places. Due to larger surface area of the plate sample, the temperature increase of the overall plate is relatively very slow than coupon sized samples.

Maximum compression strength test was performed on both coupon sized and plate sized samples exposed to both direct current intensities for two different durations of time. It has been observed that there is no noticeable change in maximum compression strength in percentage scale when compared to as-is samples. The change obtained was never above 3%. A new set of samples exposed to temperatures in oven at 85° C and 120° C for 3 and 4 hours were also tested for maximum compression strength. These samples seem to show a different trend in strength for 3 hours and 6 hour exposures to heat. However, this change is also very insignificant on percentage basis. Therefore, we can draw a conclusion that the commercial use of CFRP as resistive heating elements or substrates is not a degrading choice for strength when used for longer durations in their respective current ratings.

Glass transition temperatures indicate the level of crosslinking within a CFRP sample and the polymer strength. Therefore, any change within these temperatures when exposed to different current intensities, temperature and time exposures indicate a mechanical property change. It has been observed that the Tg values across all exposure segments haven't changed significantly as compared to their corresponding as-is Tg levels, indicating no change at all in the strength properties of the bulk polymer matrix.

TGA (Thermal gravimetric analysis) results have shown that significant weight reduction within polymers happens after 300°C for various polymer matrices (after this temperature, polymer mass depreciates drastically due to oxidation or bond scission of the backbone chemical structure) If this particular temperature is taken as the onset of degradation of the polymer, then how long does it take for a particular current intensity to reach 300 deg C can be a question of interest. Although it is easy to say experimentally (in our case) from what we found through the data that the rate of temperature increase in our samples for 0.0062 A/sq mm is from 0.1 (up to 3 hours) and 0.22°/min (for 3-6 hours). Based on the rate of 0.22°/min (assuming that this rate will remain constant further) it will take 13 hours for Epon resin 862 to start thermally degrading. The resistivity of each IM7 carbon fiber is $14.97 \times 10^{-3} \Omega \cdot \text{mm}$. Assuming that the current density is 40 A/sq inch and volume fraction of CF as 55% and fiber diameter is 5 microns the total heat generated due to i^2R loss within a square inch cube of CFRP per second is approximately 39.1 J. Assuming that there is no natural or forced convection and only conduction through the sample is considered. The thermal diffusivity will drain away some heat every second leaving some stored heat within every cube inch of CFRP. Once the stored heat exceeds the specific heat capacity (minimum heat required to raise the temperature of the sample by 1°) of the polymer matrix, the temperature starts to raise at the rate same as heat deposition rate. From this we can calculate “how long” for a given intensity of current would the polymer will start to degrade due to current induced temperature raise (begins at the onset of 300° C). Thus we will have established a relation between an independent current

intensity and its effect on life of unidirectional CFRP of a particular fiber volume ratio. A 2-D thermodynamic model consisting of a continuous heat source and a heat absorbing polymer can be formulated as a case of study. First law of thermodynamics can be applied to this problem to estimate the rate of temperature growth within the CFRP sample. The available data from these experiments can be fitted into the above predictive model to validate the rate at which each CFRP sample can reach maximum degrading temperature. Thus for different current intensities the life of polymer before it thermally degrades can be estimated. Also, the lowest value of current intensity below which the life of composite is technically infinite can also be calculated.

The question however that how much is the change within interfacial strength levels at fiber-matrix interface at a much lower scale still remains to be studied. Such an investigation is compulsory to ascertain the fact that CFRP are not degraded mechanically at all dimension scales of the material when subjected to low intensity direct electric current conduction.

REFERENCES

- [1] L. A. Momoda, "The Future of Engineering Materials - Multifunction for Performance-Tailored Structures," *Tenth Annu. symposium Front. Eng.*, 2005.
- [2] J. Bowman, B. Sanders, B. Cannon, J. Kudva, S. Joshi, and T. Weisshaar, "Development of Next Generation Morphing Aircraft Structures," *48th AIAA/ASME/ASCE/AHS/ASC Struct. Struct. Dyn. Mater. Conf.*, no. April, 2007.
- [3] C. Callosum, C. Callosum, S. Prefrontal, S. Prefrontal, C. Thalamus, and C. Thalamus, "Copyright 2002 scientific american, inc.," *Sci. Am.*, no. May, 2002.
- [4] J. P. Thomas, S. M. Qidwai, W. R. Pogue, and G. T. Pham, "Multifunctional structure-battery composites for marine systems," *J. Compos. Mater.*, vol. 47, no. 1, pp. 5–26, 2013.
- [5] P. Matic, "Overview of multifunctional materials," *Smart Struct. Mater.*, vol. 5053, no. Figure 1, pp. 61–69, 2003.
- [6] R. F. Gibson, "A review of recent research on mechanics of multifunctional composite materials and structures," *Compos. Struct.*, vol. 92, no. 12, pp. 2793–2810, 2010.
- [7] X. Luo and D. D. L. Chung, "CARBON FIBER POLYMER-MATRIX COMPOSITES AS CAPACITORS State University of New York at Buffalo," pp. 638–639.
- [8] P. Feraboli and P. Stickler, "22nd Annual American Society for composites technical conference, September 17-19, 2007 University of Washington, Seattle, WA," *J. Compos. Mater.*, vol. 43, no. 5, pp. 401–402, 2009.
- [9] T. R. Pozegic *et al.*, "Multi-Functional Carbon Fibre Composites using Carbon Nanotubes as an Alternative to Polymer Sizing," *Sci. Rep.*, vol. 6, no. 1, p. 37334, 2016.

- [10] U. S. Terminal, U. S. Terminal, E. Route, and E. Route, “Advisory Circular,” *Area*, no. January, pp. 1–4, 2005.
- [11] C. Karch and C. Metzner, “Lightning protection of carbon fibre reinforced plastics — An overview,” *2016 33rd Int. Conf. Light. Prot.*, pp. 1–8, 2016.
- [12] A. Larsson, “The interaction between a lightning flash and an aircraft in flight,” *Comptes Rendus Phys.*, vol. 3, no. 10, pp. 1423–1444, 2002.
- [13] B. Peyrou, a Chazottes, P. Q. Elias, L. Chemartin, and P. Lalande, “Direct Effects of Lightning on Aircraft Structure : Analysis of the Thermal , Electrical and Mechanical Constraints,” *J. Aerosp. Lab*, no. 5, pp. 1–15, 2012.
- [14] S. Mall, B. L. Ouper, and J. C. Fielding, “Compression Strength Degradation of Nanocomposites after Lightning Strike,” *J. Compos. Mater.*, vol. 43, no. 24, pp. 2987–3001, 2009.
- [15] A. TODOROKI and J. YOSHIDA, “Electrical Resistance Change of Unidirectional CFRP Due to Applied Load,” *JSME Int. J. Ser. A*, vol. 47, no. 3, pp. 357–364, 2004.
- [16] L. Cheng and G. Y. Tian, “Surface crack detection for carbon fiber reinforced plastic (CFRP) materials using pulsed eddy current thermography,” *IEEE Sens. J.*, vol. 11, no. 12, pp. 3261–3268, 2011.
- [17] K. Todoroki, Akira; Kobayashi, Hideo; Matuura, “Application of Electric Potential Method to Smart Composite Structures for Detecting Delamination,” *Jsme*, vol. 38, pp. 524–530, 1995.
- [18] J. B. Park, T. K. Hwang, H. G. Kim, and Y. D. Doh, “Experimental and numerical study of the electrical anisotropy in unidirectional carbon-fiber-reinforced polymer composites,” *Smart Mater. Struct.*, vol. 16, no. 1, pp. 57–66, 2007.

- [19] R. L. Sierakowski, I. Y. Telitchev, and O. I. Zhupanska, “On the impact response of electrified carbon fiber polymer matrix composites: Effects of electric current intensity and duration,” *Compos. Sci. Technol.*, vol. 68, no. 3–4, pp. 639–649, 2008.
- [20] O. I. Zhupanska, “A Study of Impacted Electromechanically Loaded Composite Plates,” no. May, pp. 1–19, 2006.
- [21] R. J. Hart and O. I. Zhupanska, “Characterization of Carbon Fiber Polymer Matrix Composites Subjected to Simultaneous Application of Electric Current Pulse and Low Velocity Impact,” no. April, pp. 1–9, 2012.
- [22] M. F. Haider, P. K. Majumdar, S. Angeloni, and K. L. Reifsnider, “Nonlinear anisotropic electrical response of carbon fiber-reinforced polymer composites,” *J. Compos. Mater.*, p. 21998317719999, 2017.
- [23] D.-Y. Yoo, I. You, and S.-J. Lee, “Electrical Properties of Cement-Based Composites with Carbon Nanotubes, Graphene, and Graphite Nanofibers,” *Sensors*, vol. 17, no. 5, p. 1064, 2017.
- [24] M. Miller and P. Feraboli, “Electrical Characterization of Electrified Composite Plates,” no. April, pp. 1–10, 2008.
- [25] PHILIP ROGERS, “EFFECTS OF NANOCCLAY ON CARBON FIBER REINFORCED PLASTICS AFTER ENVIRONMENTAL DEGRADATION” 2011.
- [26] K.-T. Hsiao and D. Heider, *Vacuum assisted resin transfer molding (VARTM) in polymer matrix composites*. Woodhead Publishing Limited, 2012.
- [27] I. Y. Telitchev, R. L. Sierakowski, and O. I. Zhupanska, “Low-Velocity Impact Testing of Electrified Composites: Part II—Experimental Setup and Preliminary Results,” *Exp. Tech.*, vol. 32, no. 3, pp. 53–57, 2008.
- [28] P. E. Deierling, “Electrical and thermal behavior of Im7 / 977-3 Carbon fiber polymer matrix composites subjected to time-varying and steady electric currents,” 2010.

- [29] A. N. Cycles, F. Webs, W. Sea, and E. Report, "q 2006 by Taylor & Francis Group, LLC," pp. 466–472, 2006.
- [30] M. A. Tudela, P. A. Lagace, and B. Wardle, "Buckling Response of Transversely Loaded Composite Shells, Part 1: Experiments," *AIAA J.*, vol. 42, no. 7, pp. 1457–1464, 2004.
- [31] C. Materials and M. S. Uiiiwrsiry, "Fiber-Matrix Adhesion and Its Effect on Composite Mechanical Properties : Tensile and Flexure Behavior of Graphite / Epoxy Composites," no. 3, pp. 310–333, 1991.
- [32] T. W. Tamulevich, "The significance of glass transition temperature on epoxy resins for fiber optic applications," *Proceeding Integr. Packag. Optoelectron. Devices*, vol. 703, pp. 59–64, 1986.
- [33] A. Yousefi, P. G. Lafleur, and R. Gauvin, "Kinetic studies of thermoset cure reactions: A review," *Polym. Compos.*, vol. 18, no. 2, pp. 157–168, 1997.
- [34] J. Zhou and J. P. Lucas, "Hygrothermal effects of epoxy resin. Part II: Variations of glass transition temperature," *Polymer (Guildf)*., vol. 40, no. 20, pp. 5513–5522, 1999.
- [35] N. D. Danieley and R. L. Edward, "Effects of curing on the glass transition temperature and moisture absorption of a neat epoxy resin," *J. Polym. Sci.*, vol. 19, pp. 2443–2449, 1981.

VITA

Ravi Raja Naidu Akula Venkata

Candidate for the Degree of

Master of Science

Thesis: EFFECT OF LOW CONSTANT DIRECT CURRENTS ON MECHANICAL QUASI-STATIC RESPONSE OF A CARBON FIBER POLYMER MATRIX COMPOSITE.

Major Field: Mechanical Engineering

Biographical:

Personal Data:

Born in Andhra Pradesh, India January 8, 1989.

Education:

Completed the requirements for the Master of Science in Mechanical and Aerospace Engineering at Oklahoma State University, Stillwater, Oklahoma in May,2018.

Completed the requirements for the Bachelor of Science in Mechanical Engineering at Vasavi College of Engineering, Hyderabad, India,2010.

Experience:

Graduate Research Assistant in Mechanics of Advanced Materials Laboratory (MAML), Oklahoma State University,2016-2018.

Graduate Teaching Assistant in Mechanics of Advanced Materials Laboratory (MAML), Oklahoma State University, 2016-2018.

Research Engineer at Hyundai Motor India Pvt Ltd, Hyderabad, India. 2010-2015.

Professional Memberships:

Student member with American Society of Mechanical Engineers (ASME).

